Improved Classification Accuracy of Four Class FNIRS-BCI

Author

Muhammad Saad Bin Abdul Ghaffar

Reg. Number: 00000276187 MS - 18 (MTS)

Supervisor

Dr. Umar Shahbaz Khan

DEPARTMENT OF MECHATRONICS ENGINEERING

COLLEGE OF ELECTRICAL & MECHANICAL ENGINEERING

NATIONAL UNIVERSITY OF SCIENCES AND TECHNOLOGY

ISLAMABAD

JUNE, 2020

Improved Classification Accuracy of Four Class FNIRS-BCI

Author

Muhammad Saad Bin Abdul Ghaffar

Reg. Number 00000276187 MS – 18 (MTS)

A thesis submitted in partial fulfillment of the requirements for the degree of

MS Mechatronics Engineering

Thesis Supervisor:

Dr. Umar Shahbaz Khan

Thesis Supervisor's Signature: _____

DEPARTMENT OF MECHATRONICS ENGINEERING

COLLEGE OF ELECTRICAL & MECHANICAL ENGINEERING

NATIONAL UNIVERSITY OF SCIENCES AND TECHNOLOGY, ISLAMABAD

JUNE, 2020

Declaration

I certify that this research work titled "*Improved Classification of Four Class FNIRS-BCI"* is my own work. The work has not been presented elsewhere for assessment. The material that has been used from other sources it has been properly acknowledged / referred.

Signature of Student

Muhammad Saad Bin Abdul Ghaffar

00000276187 MS-18 (MTS)

Language Correctness Certificate

This thesis has been read by an English expert and is free of typing, syntax, semantic, grammatical and spelling mistakes. Thesis is also according to the format given by the university.

Signature of Student

Muhammad Saad Bin Abdul Ghaffar

00000276187 MS-18 (MTS)

Signature of Supervisor

Copyright Statement

Acknowledgements

I am thankful to Allah Subhana-Watala to have guided me throughout this work at every step and for every new thought which You setup in my mind to improve it. Indeed, I could have done nothing without Your priceless help and guidance. Whosoever helped me throughout the course of my thesis, whether my parents or any other individual was Your will, so indeed none be worthy of praise but You.

I am profusely thankful to my beloved parents who raised me when I was not capable of walking and continued to support me throughout in every department of my life.

I would also like to express special thanks to my supervisor Dr. Umar Shahbaz Khan for his help throughout my thesis and also for Advance Embedded System course which he has taught me. I can safely say that I haven't learned any other engineering subject in such depth than the one which he has taught.

I would also like to pay special thanks to Dr. Nouman Naseer (Air University) for his tremendous support and cooperation. Each time I got stuck in something, he came up with the solution. Without his help I wouldn't have been able to complete my thesis. I appreciate his patience and guidance throughout the whole thesis.

I would also like to thank Dr. Nasir Rashid, and Dr. Mohsin Islam Tiwana for being on my thesis guidance and evaluation committee and express my special Thanks to my close aid Rayyan Azam Khan and Sir Farzan Majeed Noori for their time, continuous support and cooperation.

Finally, I would like to express my gratitude to all the individuals who have rendered valuable assistance to my study.

Dedicated to my exceptional parents and adored siblings whose tremendous support and cooperation led me to this wonderful accomplishment

Abstract

Experimentation and analysis in brain-computer interface (BCI) has increasingly been receiving quite some consideration as a substitute communication possibility for patients who are severely paralyzed in the last few years. To measure brain activities using optical signals a fairly new and non-invasive brain imaging tool can be put to test know as Functional near-infrared spectroscopy (fNIRS). Comparability low cost, safety, portability and wear ability are some of the main advantages of imaging of brain using this non-invasive modality. We have applied this relatively new non-invasive fNIRS technique to make an image of brain activities during four different mental tasks. These tasks include Mental Arithmetic (MA), Motor Imagery (i.e. Left-Hand and Right-Hand Motor Imagery) and Rest. fNIRS data used is an open access dataset of 29 individuals which was collected by Continuous-wave imaging system (NIR Scout NIRx GmbH, Berlin, Germany) with the sampling frequency of 10 Hz. In this research Data synchronization is performed before the data is preprocessed. Usual preprocessing is done using Butterworth filter of 4^{th} order to minimize or eliminate any unwanted signal distortion. After that an extensive signal analysis is done in which Six different statistical features (Signal Mean (SM), Skewness (SK), Kurtosis (KR), Standard Deviation (SD), Signal Peak (SP), and Signal Variance (SV)) are obtained in the time domain and 13 MFCC (Mel Frequency Cepstral Coefficients) features are obtained from the frequency domain. After the preprocessing and signal analysis of data our results shows hemodynamic behavior of multiple patterns during the tasks performed. These unique patterns of hemodynamic behavior can be used to differentiate and distinguish different task. Separate Classification analysis is performed on each domain features. We were able to compare, differentiate and distinguish the brain signal activities captured while performing 4 different tasks using 3 different classifiers i.e. Linear Discriminant Analysis (LDA), Support Vector Machine (SVM) and K Nearest Neighbor (KNN). The average classification accuracy of above 90% is achieved from K Nearest Neighbors (KNN) using the time domain features and same accuracy is achieved from Support Vector Machine (SVM) using the frequency domain features.

Key Words: *Multiclass Brain–computer interface (BCI), fNIRS based Brain-Computer Interface, Functional Near-Infrared Spectroscopy, Mel Frequency Cepstral Coefficient (MFCC) Mental Arithmetic, Motor Imagery, Four Class*

Table of Contents

List of Figures

List of Tables

1. INTRODUCTION

To develop a brain-computer interface (BCI) system you need to have an introductory knowledge and some motivation. This chapter consist of some basic knowledge of BCI, its requirements and some real-world applications, moving towards end with problem statement, research objective and research justification. At the end a planned outline of this thesis report is given.

1.1 Motivation

Brain computer interface (BCI) systems enable people with limited motor functions to activate an external device (e.g., a neuro-prosthesis or a wheel chair etc.) by sending command through brain signals rather than muscular signals. This can affectively improve quality of their lives by reducing dependence on others [1], [2], [3] and [4]. The hemodynamic behavior of the brain, is measured by optical signals using Functional Near Infrared Spectroscopy technique in diverse environments and require an easy to handle simple, inexpensive and portable equipment [1]. BCIs are built on the principle that motor movement or cognitive information is represented by hemodynamic response generated due to neuronal activity inside the brain. This response can be recorded and then can be used to control an external device [5]. BCI systems are attracting a wide range of applications as rehabilitation measure for physically impaired people [6], [7] and [8]. Modern day challenge demands to improve the usefulness of BCI systems by increasing the classification accuracy of brain signals for different intended motor movements. This can be achieved by experimenting with selection of frequency band, feature extraction techniques, selection of FNIRS recorded channels with maximum intention information and finally a robust classification algorithm. Keeping in view the modern technology and specially the humane aspect BCI has emerged as an important research area for two decades.

The real-world applications for BCI are cursor control of a desktop computer [9], control of a car driving virtual simulator [10], web browsing and multimedia control application [11],

control of a wheelchair [12], gaming [13] etc. These applications however, demand high accuracy and high computational power and gaining the attraction of researchers.

Communication interface development with brain signals has proved to be very challenging. These challenges are related to usability of the system and are technical in nature [14]. One of the major limitations of user acceptance is the laborious training that is an essential part of class discrimination [15]. This can be overcome with the help of single trial training instead of multi-trial training, and put the burden on subsequent components on BCI system using adaptive zero training classifiers. Towards technical aspect non-linearity, non-stationarity and noisy nature of data is the main challenge [16], [17]. In BCI systems multiple channels are used for recording data, to achieve high spatial resolution, but this leads to a high dimensionality curse. Presence of noise (artifacts) in brain signals affect the quality of signals with low signal to noise ratio (SNR). To achieve better results from BCI systems increase in SNR can be achieved by applying artifact removal techniques [18]. Frequency band filtering helps in reduction of line noise (artifact) and also provides a selection of task related frequency range.

Interpretation of user's intent correctly warrants the separation of signals into multiple classes. A valid choice of separation of brain signals into multiple classes is the machine learning techniques. The filtered data is presented to machine learning algorithms for training, validation and testing. The researcher's intent and spirit are to achieve the separation of multiple classes with highest percentage accuracy.

1.1.1 Brain Computer Interface (BCI)

BCI technology is a powerful tool to communicate between the brain and computer. The complementing process between the brain and computer leads the system to drive any actuator or external device [1]. BCI does not involve any muscular movement of the body for accomplishing any movement of external device, thus creating a channel of understanding between the user and its surroundings. This communication channel is activated with the help of user's mental activity and does not involve neuromuscular system of human body [19]. Brain signals are considered to provide distinct information about the brain activity. Moreover, these distinctive brain patterns help in identifying human intention of performing any task. Identification of these intentions is

performed by a computer using signal features and classification techniques and subsequently generate signals to activate an external device. Figure 1. shows an overview of a BCI system [20].

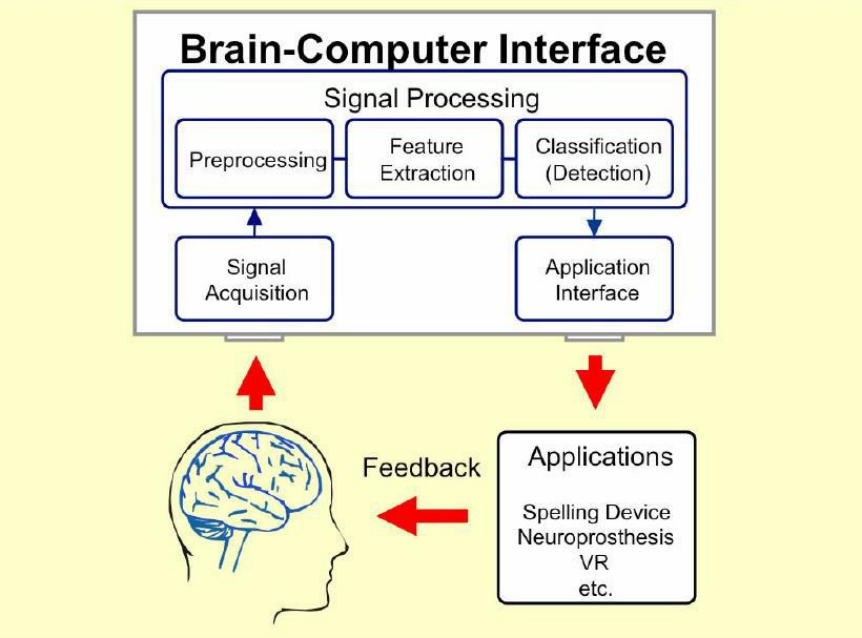

Figure 1. A typical BCI System [20]

1.1.2 Brain Anatomy

All mammals have brains but human is gifted with a brain that has the best developed and largest cortex as compared to other mammals. Cortex is the part of brain in which neural activity related to abilities like complex reasoning, speech and language etc., is executed. This activity and processing distinguish humans from other mammals. Moreover, the cortex consists of two hemispheres called right and left hemispheres. Humans can be right hand or left hand dominant and depending upon the dominance each hemisphere possesses specific abilities. For example, a right-handed person will use the right hemisphere during recognition of geometric patterns, spatial orientation, use nonverbal memory and recognition of non-verbal noises [22]. For the same person, the left hemisphere will be more active during recognition of letters and words, use verbal memory and auditory perception of words and language. Each hemisphere is further divided into five regions which are called lobes. These lobes perform different processing related to human activity through neuron firing to carry out certain task. Human brain consists of five well defined lobes

called frontal lobe, central lobe, parietal lobe, occipital lobe and temporal lobe. Frontal and central lobes plan and execute motor movements, parietal lobe is responsible for sense of touch, occipital lobe processes information related to vision and temporal lobe deals with auditory information and processing. Figure 2. shows the anatomical distribution of lobes and cortex of the human brain [21].

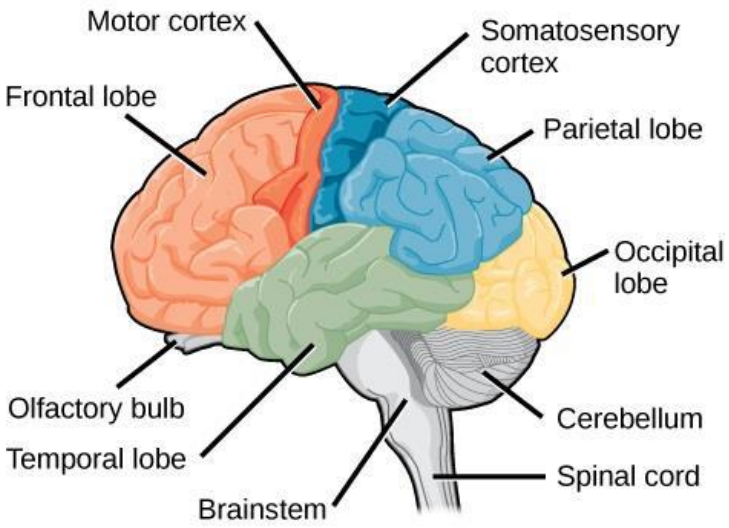

Figure 2. Brain partition with regions [21]

1.1.3 Components of a BCI System

Primarily, BCI system aims at recording of signals from brain and interpret these signals with highest classification accuracies into a command of activating an actuator over a communication channel. Four basic components of a BCI system are enumerated as under: -

- Sensors for signal recording/acquisition from brain.
- Signal processing unit for preprocessing of acquired signals by selecting the desired frequency band and removal of artifacts.
- Feature extraction unit generates the specific characteristic of the signal and also helps in reduction of data size.

- The classifiers which translate the produced features into device commands.

BCI can be classified into three types according to sensor placement for recording brain signals i.e. (i) Invasive BCI, (ii) Partially Invasive BCI and (iii) Non-Invasive BCI. The first two involve surgical procedure for placement of electrodes (sensors) for signal recording and the third one requires placement of sensors at the scalp for recording. The third one is the most used procedure for signal recording due to the obvious reason of avoiding surgical procedure. The quality of signals in the first two types is far superior to the third as it is less contaminated with any kind of electrical interference and any other organ artifacts.

Performance of a BCI system will be affected and depends upon signal to noise ratio (SNR) of the digitized signal. Present day BCI features represent brain events, which can be identified according to the firing of specific cortical neurons in the sensorimotor cortex area. For classification of user intent, the processing of signals can be done online or offline. In an online system the processing is done in real time and user intent is transformed in real time. While in an offline system the data is recorded and then its processing and classification is done offline after extracting features and decreasing the dimensions. Online BCI is a bigger challenge as compared to offline system as more computational power is required to first process the signals and then classify in accordance with user intent. The offline processing approach is a post processing approach in which maximum precision and accuracy is achieved.

1.1.4 Application of BCI System

Over a period of time, BCI systems have contributed in various fields of research and its application. These systems have been applied and sought out their way inside medical applications, neuro-ergonomics and smart environment [23], neuro-marketing and advertisement [24], education and self-regulation [25], games and entertainment [26] and security and authentication [27]. The application areas are shown in Figure 3.

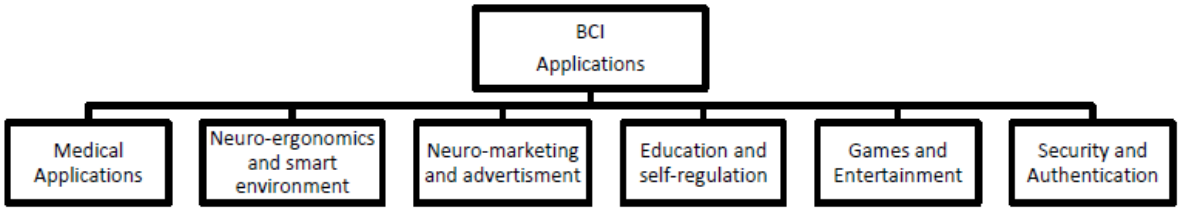

Figure 3. Applications of BCI

1.1.4.1 Medical Applications

Health care has always been an area of research for the scientists and researchers. The ingress of engineers into the biomedical engineering field has increased the pace of research manifolds. BCI is one of the well-known areas of interest for collaborative research in field of biomedical engineering. A few of the researches and its application in this area are discussed below: -

- **Prevention of Accidents**

  The main cause of death and serious injuries are attributed to traffic accidents [28]. Analyzing the cause and prevention has been a key area of research for safety of mankind. Generally, the concentration level of driver is affected due to long hours of monotonous drives over the highways and can cause motion sickness which may lead to any unfortunate incident. The motion sickness phenomenon has been studied with the help of brain signals and measured with the help of auditory evoked potentials BCI based system [29]. Monitoring of conscious level via brain waves is not limited to drivers only, rather a study for monitoring has been done on sick people staying alone for long periods of time [30].

- **Movement of Wheelchair**

  People with disability have different levels of severity. They may be paralyzed or aged and cannot perform motions of a wheelchair at their own. Research to help out such people and increasing the comfort level of their lives the concept of automated electrical wheelchair was introduced. To further enhance the comfort level the concept to use BCI system which can translate the user intention from their brain signals into motion of wheelchair. The basic

commands which can be executed are move forward, left, right and stop [31]. Controlling a wheelchair with the help of brain signals need training in real time and can compromise the safety of patient. To help patient's training, experiments have been carried out to use virtual reality platform for safe patient training [32].

1.2 Research Objectives

1.2.1 Problem Statement

The challenge in non-invasive BCI research is to identify/classify the motor imagery (EEG signals) with high accuracy. Since these signals are person specific and diverse in nature due to his mental state, achieving high classification accuracy remains a challenge for the researcher.

"An efficient method is required for improvement in multivariate classification accuracy of non-invasive brain EEG signals for an external device."

1.2.2 Research Objectives

Goal of this study is to develop a method to correctly classify the non-invasive motor imagery (EEG signals) with highest classification accuracy. The main objectives of the research are:

- Carry out study of existing methods for classification of non-invasive brain EEG signal
- Use of intelligent techniques to develop an improved method of EEG signal classification.
- Develop an intelligent classification algorithm, capable of classifying multivariate EEG signals.
- Evaluate performance of proposed intelligent classification algorithm in comparison to the benchmark techniques.

1.2.3 Thesis Organization

This thesis has been organized in six chapters; outline of the organization is as under:

- Literature review has been included in second chapter with background studies related to classification methods. Detailed literature review of relevant classification methodologies

is presented. This chapter also includes the type of BCI systems and types of brain signals and their acquisition.

- Third chapter of the thesis describes the concept and principles of Biological Immune System (BIS) theory followed by bio inspired Artificial Immune System (AIS). AIS is further explained in detail with the help of framework to understand and correlate AIS with BIS.
- Fourth chapter comprises of the developmental stages of proposed methodology. The signal preprocessing, feature extraction, dimensionality reduction techniques and genetic algorithm (GA) based optimized negative selection classification algorithm (NSCA) are presented in this chapter. Finally, classification of multivariate EEG signals using NSCA is explained in detail.
- Fifth chapter presents the results of proposed methodology in comparison with benchmark research. Classification accuracy analysis are carried out on the same dataset as of benchmark research and analysis on one more dataset (BCI competition dataset) was also carried out for validation of results.
- Main contribution of research, recommendations and future work have been included in the last chapter of the thesis.

2. BACKGROUND

2.1 BCI System Types

BCI system by-passes the normal brain's output channels (muscles and peripheral nerves) and use direct brain signals for communication and control. The BCI user produces brain signals for mental state (preforming an imagined mental task), the neuronal activity in brain generates electrical potential that is recorded for processing by the system. Depending upon the communication of brain signals and system, the BCI systems are divided into four categories, namely: 1) Dependent and Independent BCI, 2) Invasive and Non-Invasive BCI, 3) Synchronous and Asynchronous BCI and 4) Active-reactive versus Passive BCI. The fourth category is another form of dependent and independent BCI; however, it will be explained exclusively in preceding sub-sections.

2.1.1 Dependent versus Independent BCI

BCIs can be termed as dependent or independent BCI, a dependent BCI is defined as a system in which input from some muscle is existent to produce neuronal activity for communication. Contrary to dependent BCI, independent BCI do not require any muscle control and also called as pure BCI [33]. An example of dependent BCI can be a steady state visual evoked potential (SSVEP) BCI system, that is dependent upon the muscle activity in terms of gaze control. In comparison, P300 based sensorimotor cortex rhythm based BCI does not require any muscular activity for generation of neural activity. So, an independent BCI system should be used for a person who is severely disabled and lost motor control of his muscles. However, at the same time, for healthy persons playing computer games being controlled with brain signals and motor movement, a dependent BCI system will be required [34].

2.1.2 Invasive versus Non-Invasive BCI

BCI systems are named as: invasive or non-invasive, according to the method of recording brain activity [7]. The system is said to be invasive if the sensors for recording brain activity are

placed under the skull on surface of brain through an invasive surgical procedure. Contrarily, a convenient method for recording brain activity is achieved by placing electrode on the scalp. This method is termed as non-invasive BCI system and does not require any surgical procedure. The action potentials in case of invasive BCI has higher amplitude as compared to non-invasive system, therefore, these are less prone to noise and artifacts. But at the same time, it involves a surgical procedure to place the electrodes. An electrocorticogram (ECoG) is recorded by placing electrodes under the scalp and an electroencephalogram (EEG) is recorded by placing electrodes on the surface of scalp [5].

2.1.3 Synchronous versus Asynchronous (Self-paced) BCI

In a synchronous BCI system, the user will be allowed to interact with system only during specific time period as imposed by the system. A dedicated stimulus (visual or auditory) is provided by the system to user as an indication or cue for him to start interacting with the system as desired. As soon as the indication finishes the system stops communicating with user and his intents are not processed by the system. It is mandatory for the user to perform the mental task only during that interval as the system will only react at that particular time otherwise mental tasks outside that interval with result in nothing [35]. With an asynchronous system (self-paced) the user has the liberty to communicate at his will with the system, in that he may not perform any mental task and the application will not respond. Self-paced BCI systems are close to natural systems and provide user with the flexibility to interact with system at his will, however, designing such system is very challenging as compared to synchronous system. Ideally all system should be asynchronous (self-paced) but in this case the system has to analyze the input (brain signal) continuously and determine that when the user wants to interact with application and also system has to identify as to what action user wants to perform. Due to this challenge most of the BCI systems are synchronous [36].

2.1.4 Active-reactive versus Passive BCI

In an active BCI system, the brain signals are generated by the user intentionally which are independent of the external events. These brain signals fall under category of motion intentions,

mental tasks and motor imageries. Contrary to active BCI, the brain signals generated in reaction to an external stimulus is called reactive BCI. All video, audio or pain stimuli cause generation of reactive signal in brain which can be utilized for a reactive BCI application. In a passive BCI system, any arbitrary brain activity which is neither intentional nor generated because of external stimuli is used for any object control. For example, fatigue estimation of a human being or estimation of drowsiness of a driver falls under the category of passive BCI [37].

2.2 Types of Brain Signals and Acquisition

BCI systems operate on brain signals recorded from the brain activity of subject. Many types of suitable brain activities (subject's intent) have been tried and identified for recording to activate a BCI system. As discussed above these signals (activity) can be recorded by means of electrode which can be invasive or non-invasive, moreover, these signals can be electrical potentials or other signals.

2.2.1 Neurophysiological Signals for BCI

Classification of brain activity patterns (neurophysiological signals) of a subject for one or several distinct movements with highest accuracy is the ultimate goal of BCI systems. These patterns are associated by BCI systems with respective movements and command signals are generated to perform the task with the help of external world actuators. The signals which are identifiable relatively with ease and prove to be easy for the user to control the actuator are divided into two main categories [38]. These brain activity patterns (neurophysiological signals) are also called and referred to as a mental state.

- **Evoked signals:** These signals are generated when a subject notice a stimulus generated externally and perform any mental task. Due to their nature of generation, these are called evoked potentials (EP).
- **Spontaneous signals:** These signals are generated at the will of the user voluntarily without the influence of any external stimulus. Generation of these signals is an internal cognitive process.

2.2.2 Neuroimaging

Brain physiological activity measured directly by the electrophysiological. To view structure and operation of the brain some neuroimaging techniques can be used which are functional near-infrared spectroscopy (fNIRS), electroencephalography (EEG), magnetoencephalography (MEG), electrogastrography (EGG), electrocardiography (ECG), electrogastrography (EGG), electro optography (EOG). Neuroscientists generally uses two main classes of brain imaging techniques to measure the brain activity. These are: [39].

- **Structural Imaging**

Treats brain conditions such as tumor and injury diagnosis. A structural image illustrated in figure 4. [40].

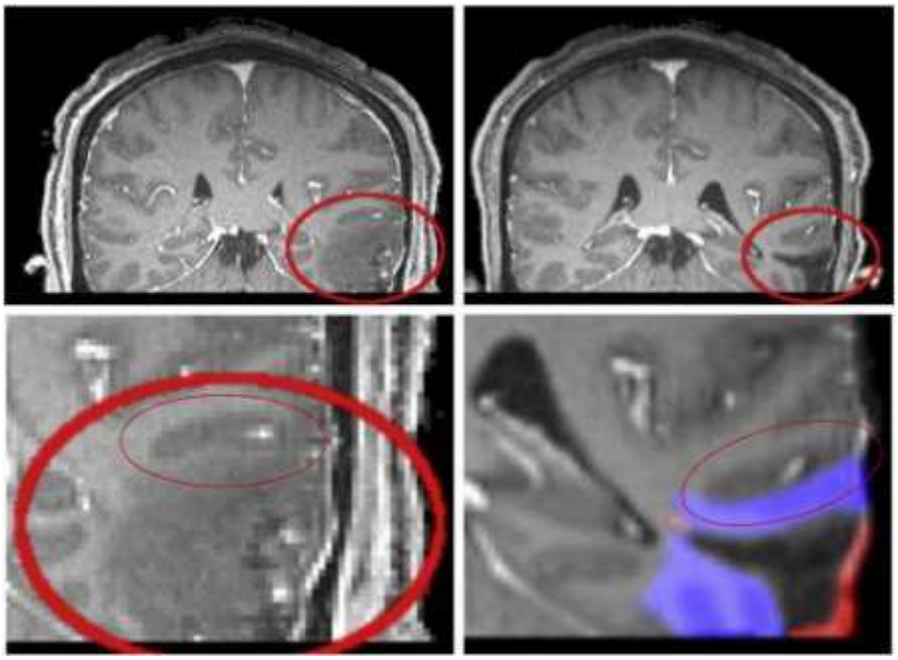

Figure 4. Structural imaging of brain [40]

- **Functional imaging**

The functional imaging is a method of detection or measurement for the effects of certain activity or event on blood flow, metabolism, absorption and local chemical composition. A functioning picture shown in Figure 5. [41].

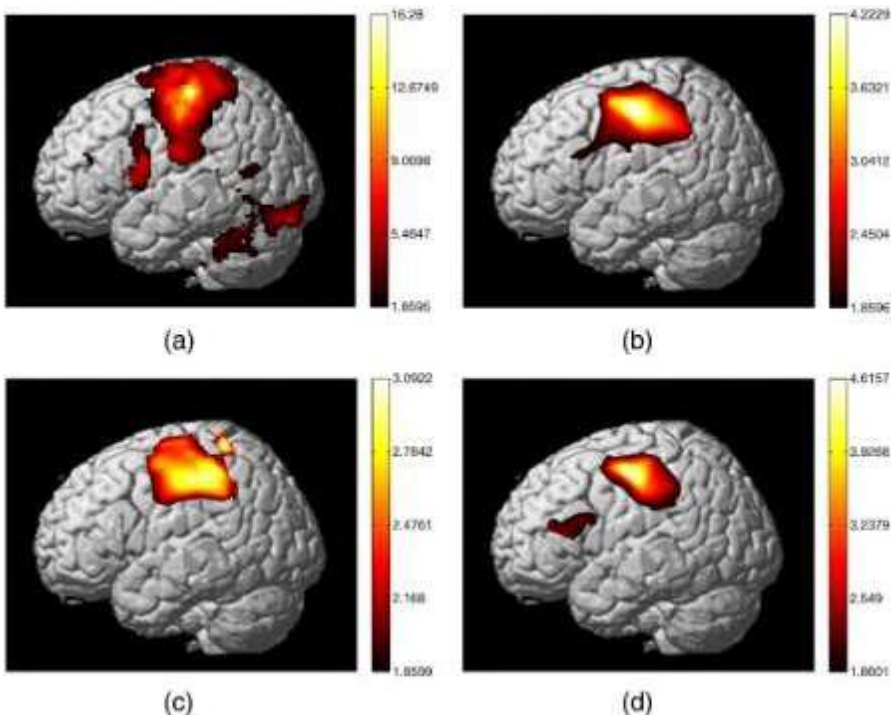

Figure 5. Functional Imaging of Brain [41]

2.2.3 Brain Signal Acquisition and Imaging

Methods for acquiring brain signals are non-invasive or invasive. Non-invasive methods, the brain signals are recorded by electrodes on the scalp. In an invasive process, electrodes are implanted directly into the gray substance which allows the acquisition of fine brain signals and poses surgical risks. Magnetoencephalography (MEG); imagery by magnetic resonance imaging (MRI), electroencephalography (EEG), tomography with positron emission (PET); computerized axial tomography (CAT); near-infrared (fNIRS) functional spectroscopy; and imagery with functional magnetic resonance imaging (fMRI). Each of us has its own advantages and disadvantages in the BCI context [26]. A brief portrayal for every method is provided below:

2.2.3.1 Magnetencephalography (MEG)

Magnetencephalography means brain pictures use magnetism. MEG (Figure 6[43]), detects brain signals through detection by electricity in the brain of magnetic fields. MEG calls for an intensive Low Noise Verstärker and expensive superconducting Quantium Interference

(SQUID) device. Ferro-Magnetic Screen Protection Room (MSR) readings should therefore isolate MEG equipment inside where SQUID is isolated by MSR. SQUID will be isolated from all magnetic externals by MSR. MEG benefits provide very high time and space resolution, which can be useful for observing events in fewer than 10 milliseconds.

Figure 6. Magnetencephalography [43]

2.2.3.2 Computerized Axial Tomography (CAT)

Computerized axial tomography is a structural technique of neuroimaging commonly known by computerized tomography. It's also referred to as the CT scan. An CT scan consists of a series of x-ray images around the head from several places. These combined images build a brain image. CT scans are not high-quality resolution, but any significant anatomical problems in the brain, such as tumors may be visualized.

2.2.3.3 Magnetic Resonance Imaging (MRI)

The use of magnetic fields and power waves with radiofrequency to the brain requires magnetic resonance imaging, or MRI. Atomic hydrogen reacts to radiation pulses by emitting energy to the magnet fields. The MRI machine receives this energy and can tell from which part

of the brain it originated. A computer can retrieve a high-space depiction of the brain through this knowledge.

2.2.3.4 functional Magnetic Resonance Imaging (fMRI)

Functional MRI or fMRI works in a similar manner to MRI but tends to focus on different approaches to oxygenized and deoxidized blood magnetic fields and radiofrequency energy. Blood-oxygen-based contrast (BOLD) is used by the FMRI (Figure 7[44]) to detect changes in brain blood flow and thus to identify brain areas which are the most active [44]. The fMRI can be imaged without something manipulating the brain activity and provides high-resolution MRI pictures concurrently with functional photographs.

Figure 7. functional Magnetic Resonance Imaging [44]

2.2.3.5 Positron Emission Tomography (PET)

Tomography with Positron emission is a type of imagery in the brain, or a PET scan. A patient is injected with a radioactive positron-emitting substance for a PET scan and gamma rays will be emitted when the electrons in the brain tissue collide. These gamma rays are identified by the PET scanner (Figure 8[45]). The PET scanner tracks blood flow across the entire brain, because the toxic material was pumped into the blood stream. The PET scanning process produces a picture

that shows the most common areas of the brain while the person is in the scanner. when this area is active the blood flux in the brain increases.

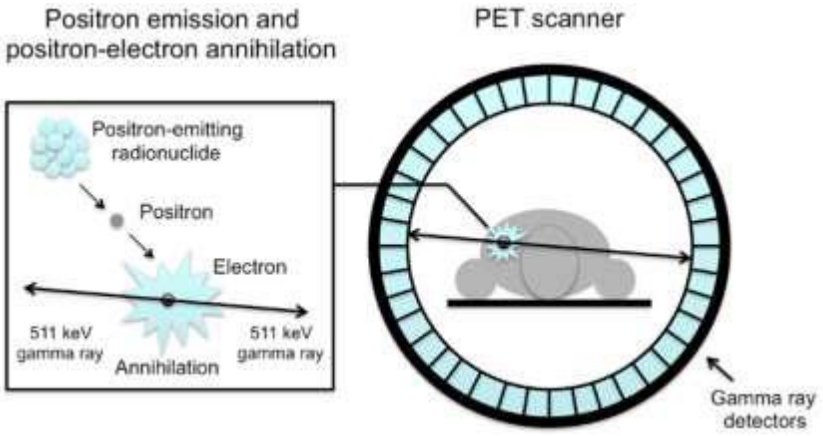

Figure 8. Positron Emission Tomography (PET) [45]

2.2.3.6 Electroencephalography (EEG)

EEG refers to electrical activity recording in the brain. If the brain information changes, the electrical flow interneurons will cause an electric field to be measured on the head surface [46]. Multiple electrodes are used in various areas of the head surface to monitor brain activity. Energetic electrical activity (Figure 9[46]) can record milliseconds and it is a powerful means of investigate different aspects of cognition, like immediate memory and perception. Low-space resolution is the biggest drawback of EEG.

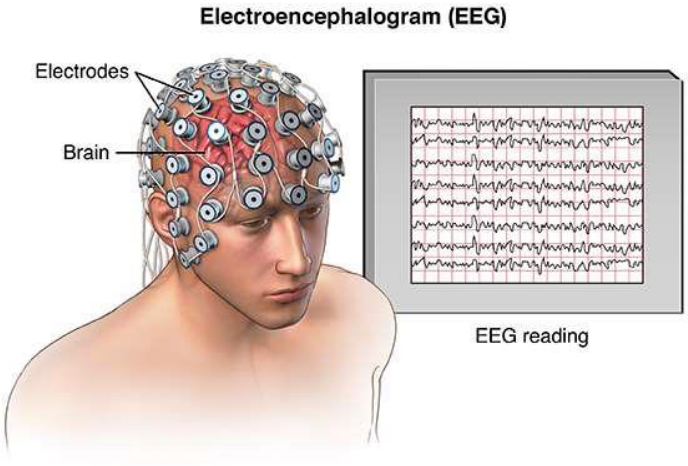

Figure 9. Electroencephalography (EEG)

2.2.3.7 functional Near-Infrared Spectroscopy (fNIRS)

FNIRS is fairly new and functional in reflecting Near-Infrared (NI) light on the scalp 's surface into its brain as the light is reflected backwards [29] by quantifying optical answers of wavelengths varied (normally 650~1000 nm). The functional maps of brain activity may be created using FNIRS. This produces pictures similar to the fMRI pictures. The spatial resolution of photos is related to fMRI and is quite high. Its main benefits are low noise, low cost, security, portability, and user-friendly compared to fMRI. Unlike EEG and MEG, his information is not sensitive to electric noise, as it represents a method of optical imaging. FNIRS measures the blood flow-alteration (hemodynamic response) caused by neuron activation [6]. Because the oxygen carrier is also hemoglobin, changes in the level of HbO and HbR might be associated with the relevant neuronal firings after neuronal activation. FNIRS uses pairs of NI lamps, NI photons fly over the head floor, disperse across brain tissues, causing multiple photon scattering. Some of these photons are removed after they pass the cortical part of the brain, which is changing chromophores (i.e. HbO and HbR). Then these stimulated photons are observed with detectors. During the application of the modified Beer-Lambert Act (23) the relationships entre the photon intensity of an incident and the photon intensity of an output can be used to measure changes in concentrations of HbO and HbR along the path of photons because there are different absorption coefficients for different wavelengths of NI light. These excited photons are then spotted by using detectors. Since HbO and HbR have different absorption coefficients for various wavelengths of NI light, the relationship between the incident photon intensity and the exiting photon intensity can be used to compute the changes of the concentrations of HbO and HbR along the path of the photons by applying the modified Beer-Lamberts law [49].

The Near Infrared Spectroscopy Concept was first developed in 1977[50] Jobsis requires the use of 3~4 cm of emitting and detecting systems. The distance is important because the only contribution to a small distance (1 cm) is from the skin, while a large distance of (5 cm) may send poor quality and unnecessary signals. Table 1 summarizes the non-invasive methods of brain signal acquisition.

Table 1. Summary of some BCIs w.r.t Data Acquisition

Data Acquisition	Signals	Pros	Cons
EEG	Electrical Activity	• Portable equipment • Easy to use	Low Topographical Resolution
MEG	Magnetic Activity	Excellent spatial and temporal resolution	• Costly and Heavy equipment • Impractical for clinics
PET	Metabolic Activity using Nuclear Meds		• Expensive equipment • Usage of Nuclear Meds
FMRI	Hemodynamic Response	Good Spatial Resolution	• Heavy Equipment • Poor temporal Resolution
FNIRS	Hemodynamic Response	• Good spatial resolution • Good temporal resolution • Portable Equipment	• Costly equipment

2.3 Data Extraction

Hemodynamic changes to blood flow can be detected by neuroactivation fNIRS. The U.S. test company defines a wavelength range for the NI from 780 nm to 2526 nm. For the NIRS as a whole NI wavelength spectrum, the range of 650-1000 nm is not possible. Figure 10 illustrates different wavelength spectrum ranges.

Figure 10. Wavelength Spectrum

Light absorption occurs because of oxyhemoglobin, deoxyhemoglobin, bulk lipids and water in this electromagnetic spectrum region. Water absorption is very small during this range. It does not have precious details. In order to identify increases in oxyhemoglobin and deoxy-hemoglobin concentrations, lipids and water are typically less absorbed. The sum of brain activity in the field can be measured. When an operation takes place, the nerves are shot. Glucose or oxygen are required in the neurons and oxyhemoglobin (HbO) gives off. When oxyhemoglobin increases and deoxyhemoglobin decreases, the supply of blood oxygen to the region increases as shown in Figure 11. The total hemoglobin (oxyhemoglobin and deoxyhemoglobin) remains constant. Some chromophores still occur in the cortex, i.e. The absorption coefficient of these chromophores is negligible for myoglobin, cytochrome and meth-hemoglobin, etc. (~650nm-100 nm) [51].

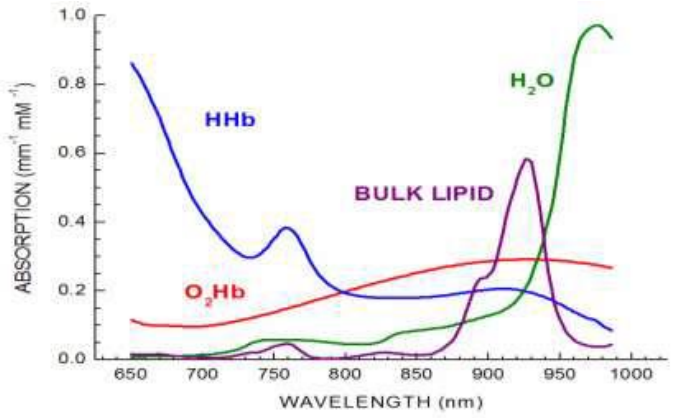

Figure 11. Absorption Coefficients of HbO & HbR

A radiation strike on the brain scatters 3 cm in the membranes of the human brain and, unlike the photons, penetrates. The ideal direction for detecting cortical activity of the mind is around 3 cm from the source to the detector distance. A banana form is used to contain 80% of the

photons observed (Figure 12). With the distance from the source detector the depth decreases, and the optical properties of the tissue depend on it. This could affect the tissue [51] if the light intensity is high.

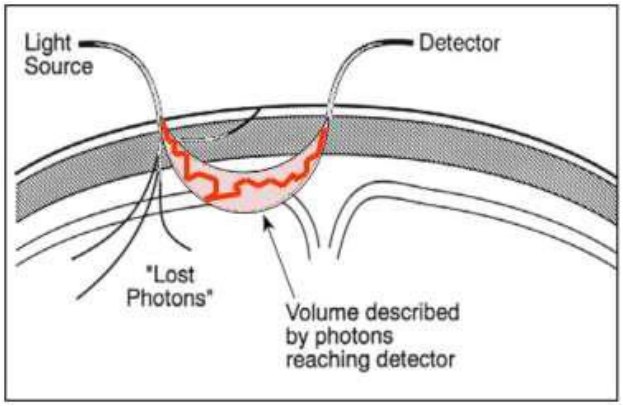

Figure 12. Path of the Photons

If light penetrates in the human brain, hemodynamic reactions, i.e. changes in the oxygenated hemoglobin and deoxygenated hemoglobin blood, are sensed. The neuron needs energy to build space for action (neuron fires). The blood vessels in the brain contain oxygenated hemoglobin. During the neuron firings leave deoxygenated hemoglobin, oxygen is withdrawn from those vessels. Blood flow increases with brain activity, thereby increasing the level of oxygenated hemoglobin. At first, the dip is happening as the HbO falls first at the onset of the cycle and then the blood flow rises. When an impulse is given to a body, neuron is set on fire before it stabilizes and this is about to happen. 21 secs. 21 secs. Figure 12[53] showed the response for hemodynamics. The pitch onset is roughly 2 seconds. The oxygenated hemoglobin concentration increases after a 2 sec delay and reaches its peak in approximately 5 to 7 seconds [52].

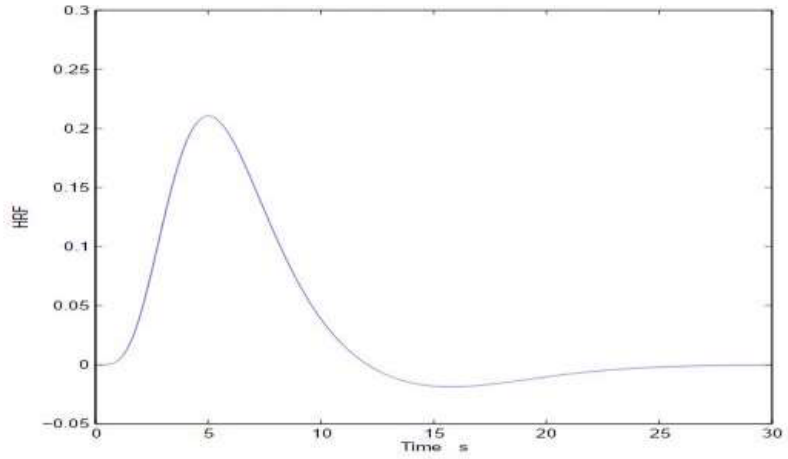

Figure 13. Hemodynamic Response of the Activity [53]

Detector distance shall be at least 2.5 ~ 3.0 cm for the access to the cortical area. When it is less than 2.5 cm from source to detector, the distance in the cortical areas is not far enough to be quantified. The detector reached could become too low if the source and detector was too far.

2.3.1 Beer Lambert Law

The Beer-Lambert Law defines the relationship between the light absorbed by the substance, concentration of the substance in the solvent and path of the light (Figure 14) [49].

$$I_{out} = I_{in} e^{-\mu_a(t) \times l} \quad (1)$$

Where

I_{out}: Intensity of light detected

I_{in}: Intensity of incident lights

$\mu_a(t)$: Mediums absorption coefficient

l: Distance between the source to the sensor

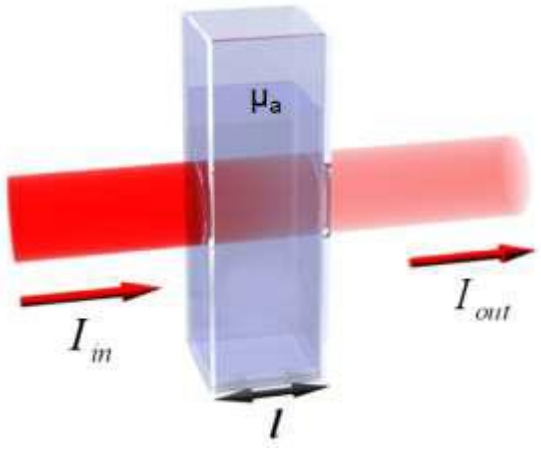

Figure 14. Beer Lambert Law Absorption

A [unit less], which is based on the wavelength β [nm] of the incident light, is the absorbance or the optical density defined as

$$A(t:\lambda) = -ln\frac{I_{out}(t:\lambda)}{I_{in}(\lambda)} = \mu_a(t:\lambda) \times l \quad (2)$$

To the brain the path of the light incident is not clear. Differential length factor should be added in order to calculate the relative concentration based on a photon path's total length. The amended law is referred to as the Modified Beer Lambert Law (MBLL).

2.3.2 Modified Beer Lambert Law

The modified law of Beer-Lambert (MBLL) forms the basis of ongoing near-infrared spectroscopy of tissue [54]. The scattering loss is regarded as constant and the tissue absorption changes evenly.

$$A(t:\lambda) = \mu_a(t:\lambda) \times l \times d(\lambda) \times \eta \quad (3)$$

Where

$d(\lambda)$: Factor of disparity direction

η: Intensity lost due to dispersion (Unknown geometry dependent factor)

Since HbO and HbR have different absorption coeffects for different NI light wavelengths, it is possible to calculate the connection between the existing photon intensity and

the photon intensity incidents $\Delta c\text{HbO}(t)$ and $\Delta c\text{HbR}(t)$ can be measured along the path of photons for the measurement of HbO and HbR.

$$\Delta A(t{:}\,\lambda) = A(t_2{:}\,\lambda) - A(t_1{:}\,\lambda) = -ln\frac{I_{out}(t_2{:}\,\lambda)}{I_{out}(t_1{:}\,\lambda)} = \Delta\mu_a(t{:}\,\lambda) \times l \times d(\lambda) \qquad (4)$$

$A(t_2{:}\,\lambda)$, $A(t_1{:}\,\lambda)$: Measured absorbance at two time points

$I_{out}(t_2{:}\,\lambda)$, $I_{out}(t_2{:}\,\lambda)$: Intensities two time points

The chromophores of the tissue consist primarily of HbO and HbR

$$\Delta\mu_a(t{:}\,\lambda) = [\alpha_{HbO}(\lambda)\Delta C_{HbO}(t) + \alpha_{HbR}(\lambda)\Delta C_{HbR}(t)] \qquad (5)$$

Where

$\alpha_{HbO}(\lambda)$, $\alpha_{HbR}(\lambda)$: HbO and HbR extinguishing coefficient, each [μM-1cm-1]

$\Delta C_{HbO}(t)$, $\Delta C_{HbR}(t)$: HbO and HbR change respectively in concentration [μM]

Replacement of equation (absorption coefficient value)

$$\Delta A(t{:}\,\lambda) = [\alpha_{HbO}(\lambda)\Delta C_{HbO}(t) + \alpha_{HbR}(\lambda)\Delta C_{HbR}(t)] \times l \times d(\lambda) \qquad (6)$$

By measuring the absorbance at two wavelengths, $\lambda 1$ and $\lambda 2$ (assume that d is constant)

$$\Delta A(t{:}\,\lambda_1) = [\alpha_{HbO}(\lambda_1)\Delta C_{HbO}(t) + \alpha_{HbR}(\lambda_1)\Delta C_{HbR}(t)] \times l \times d \qquad (7)$$

$$\Delta A(t{:}\,\lambda_2) = [\alpha_{HbO}(\lambda_2)\Delta C_{HbO}(t) + \alpha_{HbR}(\lambda_2)\Delta C_{HbR}(t)] \times l \times d \qquad (8)$$

After simplification the final term become:

$$\begin{bmatrix}\Delta C_{HbO}(t)\\ \Delta C_{HbO}(t)\end{bmatrix} = \frac{1}{l \times d}\begin{bmatrix}\alpha_{HbO}(\lambda_1) & \alpha_{HbR}(\lambda_1)\\ \alpha_{HbO}(\lambda_2) & \alpha_{HbR}(\lambda_2)\end{bmatrix}^{-1}\begin{bmatrix}\Delta A(t{:}\,\lambda_1)\\ \Delta A(t{:}\,\lambda_2)\end{bmatrix} \qquad (9)$$

2.4 Pre-Processing

When the fNIRS data has been extracted, artifact removal (de-noising) is the first step of preprocessing. This leads to enhance the SNR of the signal resulting in improvement of relevant information present and embedded in these signals. EEG signals are prone to be affected by artifacts (noise) which are associated with the electrical activity of movement/blinking of eyes (EOG: ocular artifacts), muscles (EMG: muscular artifacts) and rhythmic activity of heart beat (ECG: cardiac artifacts [61]). Moreover, the background brain activity is also required to be removed which is not related to signal of interest. Largely, in preprocessing the set of signals is transformed into a new set which is less affected by the influence of noise (de-noised signal). Alternatively, we may say that preprocessing is performed with an aim to increase SNR of signal. In BCI system applications, increase in SNR of EEG signal can be achieved by applying simple temporal and spatial filtering techniques.

2.4.1 Temporal Filtering

Simple temporal filters are used to extract a frequency band of interest form the signal, such as low-pass or band-pass filters. The application of these filters allows us to extract the frequency range according to the brain rhythm of interest. This filtering technique can remove the undesired band of frequencies such as variation in EEG signal due to electrode polarization (slow variations) and powerline interference (50 Hz). In other words, temporal filtering reduces the influence of frequencies lying outside the region of interest. Most common filtering techniques used for temporal filtering are, 1) Discrete Fourier Transform (DFT), 2) Finite Impulse Response (FIR) or 3) Infinite Impulse Response (IIR) filters.

2.4.2 Spatial Filtering

Spatial filters isolate and spatial information present in the signal by virtue of placement of electrode over the scalp. This can be achieved by assigning larger weights to signal acquired by electrodes placed on area of interest and smaller weights to signals acquired by electrodes placed elsewhere [55]. A simple most type of spatial filter can be formulated by considering only those

electrodes which are placed over region of interest on the scalp. We can ignore all other electrode signals as these are only contributing towards adding noise in the form of background activity to the signal not relevant to targeted BCI.

2.5 Feature Extraction

2.5.1 Statistical Features

In order to attain high classification accuracy through a selected classifier, features play an important part in a given BCI system. As a researcher, the decision to use a particular feature for classification will depend upon the knowledge about the properties of the feature for optimum performance of classifier. Since fNIRS signal is time variant so feature extraction and selection becomes vital for performance of a BCI system. Researchers have used a variety of statistical features for increased classification accuracy of a BCI system. Some of the statistical features being used are listed under:

- Signal Mean
- Signal Peak
- Skewness
- Kurtosis
- Variance
- Standard Deviation

2.5.1.1 Signal Mean

(SM) Signal Mean, the derivation was:

$$SM = \frac{1}{N}\sum_{i=1}^{N} Z_i \tag{10}$$

where N is the total data points and Zi = $\Delta c_{HbO}(t)$, across every data point.

2.5.1.2 Skewness

(SK) Signal Skewness was derived from the dissymmetry of signal mean corresponding to its normal distribution:

$$Skew(Z) = E\left[\left(\frac{Z-\mu}{\sigma}\right)^3\right] \quad (11)$$

where E is predicted value of Z and standard deviation of Z is defined by σ.

2.5.1.3 Kurtosis

(KR) Kurtosis is a measure of whether the data is heavily outliers or lightly outliers relative to a normal distribution. That is, data sets with high kurtosis tend to have outliers. Data sets with low kurtosis tend to lack of outliers. Kurtosis is computed by:

$$Kurt(Z) = E\left[\left(\frac{Z-\mu}{\sigma}\right)^4\right] \quad (12)$$

where E is predicted value of Z and standard deviation of Z is defined by σ.

2.5.2 MFCC Features

The mel frequency cepstral coefficients (MFCCs) is a frequency domain function used for this analysis. MFCCs are commonly used in the transmission of voice signal due to their robustness. Their features of handling non-linear frequency (by translating to mel frequency scale) and their unrelated characteristics are also very common. Take into account the non-stationarity of the fNIRS signals, sound and fNIRS are identical. This relation has been found by us and MFCCs have been used for the extraction of fNIRS signals. By following actions MFCCs can be obtained.

- Calculate the fast Fourier transform (FFT) of a windowed signal.
- Convert the powers of spectrum into mel scale using mel filter bank.
- Calculate the log power of mel frequencies.
- Calculate the discrete cosine transform (DCT) of mel log powers.
- Calculate MFCCs as the amplitudes of the resulting spectrum.

Figure 15 shows the process flow of extraction of MFCCs from EEG signals.

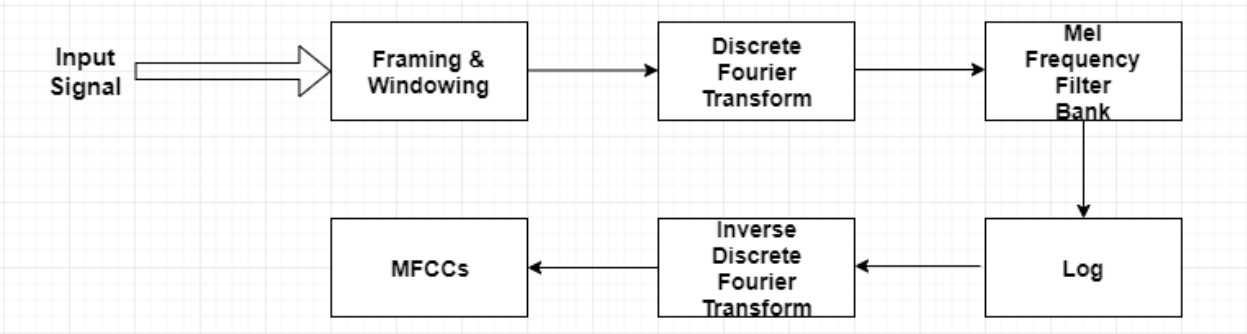

Figure 15. MFCC Extraction Flow Process

2.6 Classification

Classification consists of predicting the certain outcome based on given input. It is a systematic approach to building classification models from input data [35]. The process involves two phases:

- Learning phase
- Classification phase

In the learning phase, training data analyzed by classification algorithm is used to produce the unknown results. Test data is used to estimate the accuracy of classification. This algorithm analyzes the input to produce the prediction.

In the brain-computer interface, different brain patterns (signals) which are generated by the person can be identified using classification techniques. These identified signals are then used as a control commands for different applications purposes. In fNIRS-BCIs, such identification is performed by using classification methods to separate different mental tasks (brain signals). Some classification methods used in fNIRS-BCIs are:

2.6.1 Linear Discriminant Analysis (LDA)

LDA, also called as Fisher's LDA (FLDA) after the name of its founder, uses hyperplanes to separate the classes of data being represented in more than one dimension [58], [59]. Figure 15 shows the hyperplane distinguishing two classes of data vectors with LDA.

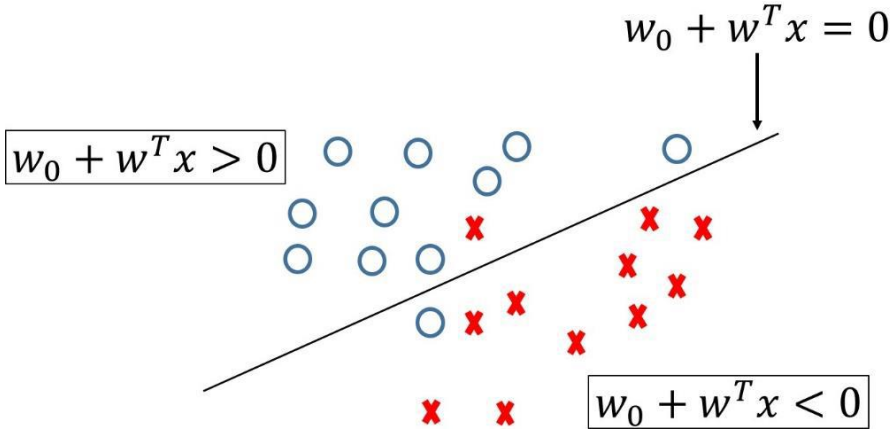

Figure 16. Hyperplane Separating Two Classes [59]

LDA assumes that data is normally distributed and both classes have equal covariance. The hyperplane separating the classes, is obtained as such that the projection of data onto the plane minimizes the within class variance and maximizes the between class variance. If the number of classes are more than two, (N>2) more than one hyperplane will be used for separating the classes. For this approach "one verses rest" strategy is used for multiclass problem by separating one class from all others. LDA is a stable classifier with very low computational complexity and this quality leads to its suitability for BCI applications. LDA has been used for BCI systems working on motor imagery with success, however, the main disadvantage of LDA is its linearity while being used for a complex non-linear data that results in low accuracy results. To improve classification accuracy and reduction of error, a regularized Fisher's LDA (RFLDA) has been suggested by Blankertz et. al. This model includes a regularization parameter C that allows or penalize the classification error on training dataset. The regularized trained classifier shows better performance if outliers are present in the data and exhibits better generalization capabilities [60].

2.6.2 Support Vector Machine (SVM)

Linear-SVM also construct a discriminant plane to identify the classes, however, the hyperplane is selected such that it maximizes the margin with nearest data point. This

maximization of margin increases the generalization capability of classifier [59]. Figure 16 shows the hyperplane distinguishing two classes of data vectors with SVM.

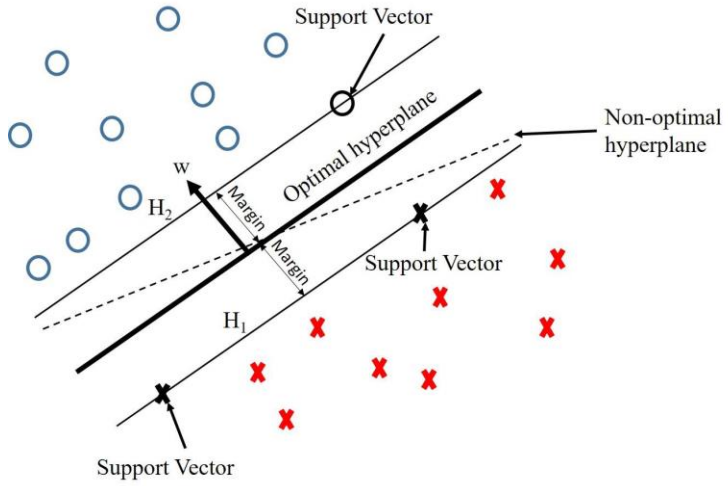

Figure 17. SVM using optimal Hyperplane [59]

2.6.3 K- Nearest Neighbors (KNN)

K-NN classifier uses the technique of assigning the feature vector (unseen data point) to a dominant class among its ‘k’ nearest neighbors within the training set. For BCI applications, the technique of calculating metric distance is used for determining the nearest neighbors. A higher value of ‘k’ with sufficient training samples k-NN is capable of producing a non-linear decision boundary for classification. k-NN classifiers are not very popular in BCI classification as these are very sensitive to curse of dimensionality and lead to low performance in BCI experiments. Use of k-NN in BCI applications with low-dimensional feature vectors has better performance as compared to high dimensional space.

3. Literature Review

This chapter presents a brief review of earlier methods used to increase the classification of fNIRS based BCIs. Moreover, a benchmark paper and its comparison with this study is also explained in this chapter.

Abibulaev and An. [61] proposed that by selecting single channel base on wavelet coefficient than classify it with svm can increase the accuracy up to 90% of a 2-class system in which 4 commands can be used.

Thanh Hai et al 2013 [62] proposed a way by using the Savitzky–Golay filter to smooth the signal of right and left finger tapping experiment and then classifying using two classifiers i.e. SVM and ANN in which ANN give the best classification accuracy.

The feasibility of a three-class fNIRS — BCI which comprises the fNIRS hierarchy, corresponding to three separate cognitive tasks deliberately created, was demonstrated by Hong et al 2015[63]. At the same time, fNIRS signals were acquired from prefrontal and primary motor cortex, which correspond to mental arithmetic, right-hand motor imagery and left-hand motor imagery. A signal slope and signal average were measured at 2–7 s time window for a classification accuracy of 75.6 percent.

Naseer et al 2013[64] submitted the findings of right-handed and left-handed wrist imagery classification based on fNIRS, using the LDA as classification. Participants were instructed to imagine the movements of the right or left hand, as shown on a computer monitor, kinesthetically. In the 10 s task period and across the different windows of time within the task period, two distinct features, the signal mean (SM) and the signal slope (SS), were used to classify right and left-wrist imagery. During the entire 10-s task period, the average classification accuracies were 73.35% and 83.0% respectively and SS. Nonetheless, these accuracies increased by increasing the time interval

in the working age to 2-7 s to 77.56 percent and 87.28 percent respectively. The time frame of 2 to 7 s is the best time window size in terms of rating analysis from 6 different timeframes.

Naseer et al 2015[65] demonstrated that a practical four-class brain-computer interface for NIR spectroscopy could be implemented in a decoding manner, reacting to questions of four choices. The RMI, LMI, MA and MC functional NIR signals were "synchronously" acquired from the primary motor and the prefrontal cortices. The four cognitive tasks were classified to an average accuracy of 73.3% with SM and SS in a 2~7 s segment of the 10 s task period.

Naseer et al. 2016[66] reviewed the effects of a two-class near-infrared functional spectroscopy (fNIRS) brain / computer interface (BCI) classification using different classification methods, according to an experimental mental arithmetic job and rest. It was shown that for both 2 and 3-d dimensioned feature sets derived from $\Delta c\mathrm{HbO}(t)$ signaling in 7 subjects, ANN has the highest classification precision in the classification modes used in this study. The results of this study represent a major step forward in the continuous improvement of fNIRS-based BCI systems' classification accuracies.

The two classifiers were used to extract classification exactness of a functional, non-infrared (fNIRS) brain computer interface system (BCI) system (mentality arithmetic and rest task) classification for two classes [67]. Qureshi et al 2016 The research concludes that the classification accuracies of the classification of Artificial Neural Networks (ANN) using 2-feather combinations were higher than the nearest neighbor (KNN) classification. These classified signals can also be used to generate fNIRS control commands for BCI applications.

Naseer et al. [68] examined the effects on mental arithmetic and repository duties based on the use of different combinations of a six common functions for classifying a two-class near-infrared functional BCI (fNIRS). Combining peak to mean values of changes in oxygenated hemoglobin (HbO) and deoxygenated hemoglobin (HbR) concentrations was demonstrated to achieve the best average LDA grading findings for 2 and 3-feature sets in seven topics. These

findings represent an advance in ongoing efforts to improve the fNIRS-based BCI system classification accuracy.

A scheme was investigated for Hong et al [69] to detect initial dips in the fNIRS signals. The proposed scheme to combine the analysis of the vector-based phase, the establishment of a threshold value, and the prediction method have proved to be very effective in dealing with hemodynamics' latency. The results show that initial dips can be successfully detected and also that detection delays can be reduced using a q-step-away algorithm based on the ARMAX model. Initial dips can not only be detected but can also be classified as different phases to generate different BCI control commands. In fact, initial dips are identified promising new ways of understanding neurovascular connectivity and spatially more spatial imaging for the brain.

Qureshi et al [70] developed and evaluated a novel methodology based on an adaptive evaluation of GLM coefficients and extraction of MI vs. resting, MR vs. resting classification performance. The findings showed improved classification performance compared to the conventional fNIRS-BCI-based hemodynamic response. In addition, if a user cannot produce different brain signals for a particular mental task, the proposed methodology can enhance the classification performance.

Noori et al [71] proposed a new approach to evaluating the optimal combinations of practical near-infrared spectroscopy (fNIRS)-based brain and computer (BCI) interface with hybrid genetic algorithm (GA)-support-vector machine (SVM). The introduction of GAAM effectively resolves problems in the selection of high-dimensional data by conventional methods of genetic algorithm with aggressive mutation. In this report, four different time windows (0-10 s, 11-20 s, 6-15 s and 0-20 s) extracted features. We concluded that hybrid GA-SVM allows for efficient function selection with classification accuracies above 91% for the 11-20s time window.

In order to implement a gait control for a lower limb, Khan et al [72] aim to use an optimal filter and classifier to achieve maximum precision in some details. Six filters were implemented

with the five classification systems of QDA, LDA, SVM, KNN and NB to exclude physiological and instrumental noises (e.g., Kalman, Wiener, Gaussian, hemodynamic response (hrf), Band-pass, Finite Impulse response (FIR). Six-functional (i.e. SS, SP, SM, KR, SV, SK) combinations have been used for brain signal classification. The SVM classifier with hrf filter has a mean accuracy of 75 percent.

4. Material and Methods

4.1 Subjects

Five right-handed healthy male subjects participated in this study with an average age of 28 years. All of the five subjects are free from any sort of brain related diseases. All subjects have previous record of performing fNIRS based experimentation. They have given the written consent and the experiments were performed according to latest Declaration of Helsinki. The data of above-mentioned subjects are taken from Open Access Dataset for EEG+NIRS Single-Trial Classification and then rearranged it to use as a multiclass fNIRS-BCI [75].

4.2 Data Acquisition

Near-infrared light of wavelength ranging from 660~1000nm is used that passes through the skull to detect the oxy hemoglobin (HbO) and deoxy hemoglobin (HbR) present in the cortical areas of brains by the optical imaging modality i.e. fNIRS. Oxy and Deoxy hemoglobin has a certain absorption coefficient to absorb certain amount and intensity of light. Some of the photons of the near infrared light are absorb and some are reflected back and are detected by the detector placed on the skull. The detectors measure the intensity of photons reflected back. Modified Beer-Lambert Law is applied to measure the concentration changes in HbO and HbR.

Dataset used is collected by Continuous-wave imaging system (NIR Scout NIRx GmbH, Berlin, Germany), to collect the brain signals at 10 Hz sampling rate. Two wavelengths i.e. 760 and 830nm are used by this system. An emitter-detector separation of around 3cm is suggested in the literature to measure hemodynamic response signals from the Cortical areas. 1cm or less separation might result in the contribution of skin layer only whereas greater than 5cm will result in weak or unusable signal. To get the signal from each subject's prefrontal cortex and motor cortex during MA and MI task total of thirty-three physiological channels are used consisting of 11 sources and 15 detectors. The placement of electrode is shown in Fig. 3 in which Black squares are the near infrared light source and Gray square is a detector and black lines constitute a single channel.

4.3 Experimental Paradigm

A large screen is present in front of subjects sat on a comfortable chair on which instruction was given before every task. The experiment is divided into three sessions of each of the 4 tasks left hand MI, right hand MI, MA and baseline tasks. Each session consists of a 60 sec pre experiment rest and the post experiment rest. Each session consists of 20 trails which comprise of 2 sec visual instruction of the task to perform and the sequence in which it is performed. The task period was10 sec for each task and each task is followed by 15 to 17 sec of rest period. The experiment did not include the pre-rest and post-rest after a trail is completed. Fig. shows the schematic diagram of the experimental paradigm.

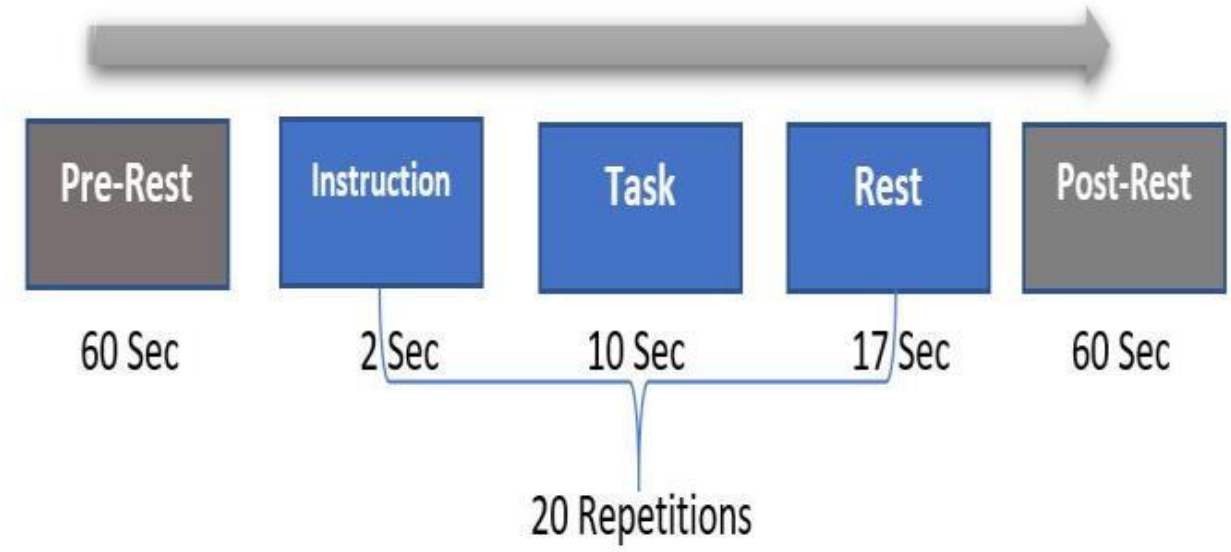

Figure 18. Experimental Paradigm

4.4 Channel Configuration and Optodes Placement

In the NIR experiment, the placement of optode is essential to ensure that photons travel through the activated area. It is very important to distance an emitter and a detector because it affects signal quality and penetration depth. At the midpoint between the emission and the detector, the maximum penetration depth is considered. In the prefrontal cortex and cortex, a total of 12

emissions and 18 detectors was used to detect mental and motor imaging signals, which included 33 channels in their configuration. Prefrontal cortex is the brain region most used in fNIRS based BCI systems because it involves less movement artifacts and signal attenuation as a result of the hair slippage. In order to obtain the highest quality signal and maximum information from it, the distance between the transmitter and the detector plays an important role. The distance between emitter and detector is usually 3~4 cm in fNIRS based BCI systems, as shown in Figure

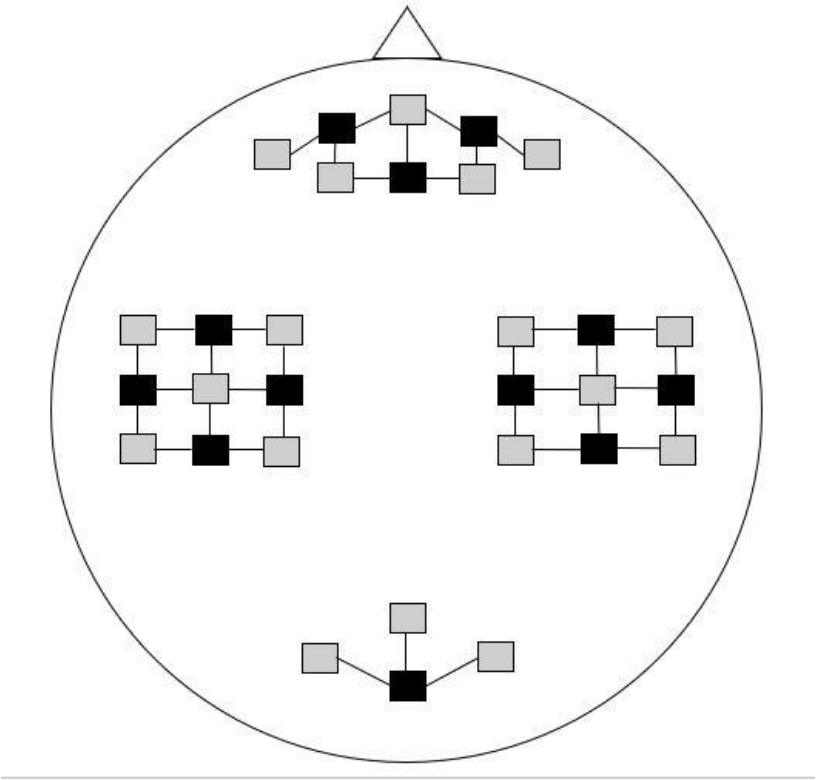

Figure 19. Optodes Placement Map

4.5 Signal Preprocessing

For the fNIRS signal processing, the first evaluations were carried out using Modified Beer Lambert law to evaluate the deoxidation and oxyhemoglobin concentration changes (HbR and HbO). The HbO and HbR data was filtered using the Butterworth filter with the 0.01–0.3 Hz passband with a sixth-order zero-phase filter. Until the filtered signals were standardized, they were separated by means of the medium and baseline correction.

4.6 Data Synchronization

As the open access dataset, we used, is collected in 6 different set in which every set contain two class data 1, 3 and 5 contain data for Motor Imagery while 2, 4 and 6 contain data for Mental Arithmetic. Every set has data of 20 trails or repetitions. Before the raw data is preprocessed and further use, we need to convert it into purely four class datasets. As the experimental paradigm is same, subjects are same and the data is collected with same machine at same sampling frequency at the same time with same electrode placement, we can combine the data channel wise such that set 1(MI) and set 2(MA) constitute into 1 set as the trails remain same. Now the final data we obtained contain 4 classes (i.e. RHMI, LHMI, MA and Rest) in each set with 10 repetition. Fig. 5 show the data before data synchronization and Fig. 6 shows after the synchronization. Every column with the same color shows the 1 repetition and every row with same pair of color show 1 set of data.

Repeat	MI 1 Time	Y	MA 2 Time	Y	MI 3 Time	Y	MA 4 Time	Y	MI 5 Time	Y	MA 6 Time	Y
1	82720	2	81280	2	86800	2	82640	1	83040	2	81520	2
2	111200	1	109760	1	116320	1	112240	2	110480	1	109040	1
3	139680	2	137280	2	143760	1	140720	1	138000	1	136560	2
4	167200	1	164800	1	171280	2	169280	2	166480	2	165040	1
5	194640	2	193280	2	198800	2	196720	1	194000	1	193520	2
6	222160	1	221760	1	227280	1	224240	2	221440	2	223040	1
7	249680	1	251200	1	256720	1	251760	1	248960	2	251520	1
8	278160	2	279680	2	284160	2	281280	2	276480	1	281040	2
9	305600	2	308240	1	312640	1	310720	1	306960	2	308560	1
10	335120	1	337680	2	342160	2	340240	2	336400	1	336000	2
11	363600	1	365200	1	370720	1	368800	2	364880	2	363520	2
12	391040	2	393680	2	400160	2	398240	1	394400	1	392960	1
13	418560	2	423200	1	427680	1	427760	2	421920	1	421440	2
14	446000	1	452640	2	457200	2	456240	1	451360	2	449920	1
15	474480	1	482160	1	486640	2	484720	2	480880	2	479440	1
16	502000	2	509600	2	514160	1	514240	1	508320	1	506880	2
17	529520	2	538080	2	542640	2	542720	2	536800	2	535360	2
18	558960	1	565600	1	571200	1	572160	1	564320	1	564880	1
19	587440	1	594080	2	599600	2	601680	1	592800	2	592400	2
20	616880	2	621600	1	629120	1	631120	2	620320	1	619840	1

	Class	Label
Set 1	LMI	1
	RMI	2
Set 2	MA	1
	REST	2

Figure 20. Before Data Syn

Repeat	MI 1 Time	Y	MA 2 Time	Y	MI 3 Time	Y	MA 4 Time	Y	MI 5 Time	Y	MA 6 Time	Y
1	82720	2	81280	4	86800	2	82640	3	83040	2	81520	4
	111200	1	109760	3	116320	1	112240	4	110480	1	109040	3
2	139680	2	137280	4	143760	1	140720	3	138000	1	136560	4
	167200	1	164800	3	171280	2	169280	4	166480	2	165040	3
3	194640	2	193280	4	198800	2	196720	3	194000	1	193520	4
	222160	1	221760	3	227280	1	224240	4	221440	2	223040	3
4	249680	1	251200	3	256720	1	251760	3	248960	2	251520	3
	278160	2	279680	4	284160	2	281280	4	278480	1	281040	4
5	305600	2	308240	3	312640	1	310720	3	306960	2	308560	3
	335120	1	337680	4	342160	2	340240	4	336400	1	336000	4
6	363600	1	365200	3	370720	1	368800	4	364880	2	363520	4
	391040	2	393680	4	400160	2	398240	3	394400	1	392960	3
7	418560	2	423200	3	427680	1	427760	4	421920	1	421440	4
	446000	1	452640	4	457200	2	456240	3	451360	2	449920	3
8	474480	1	482160	3	486640	2	484720	4	480880	2	479440	3
	502000	2	509600	4	514160	1	514240	3	508320	1	506880	4
9	529520	2	538080	4	542640	2	542720	4	536800	2	535360	4
	558960	1	565600	3	571200	1	572160	3	564320	1	564880	3
10	587440	1	594080	4	599600	2	601680	3	592800	2	592400	4
	616880	2	621600	3	629120	1	631120	4	620320	1	619840	3

Class	Label
LHMI	1
RHMI	2
MA	3
REST	4

Figure 21. After Data Syn

4.7 Feature Extraction

Six different features were extracted in the time domain by spatial averaging all of 33 physiological channels. Besides that, 13 MFCC features were also extracted in frequency domain.

Statistical features that are extracted and used are Signal Mean (SM), Skewness (SK), Kurtosis (KR), Standard Deviation (SD), Signal Peak (SP), and Signal Variance (SV) are computed for the 4 tasks.

(SM) Signal Mean, the derivation was:

$$SM = \frac{1}{N}\sum_{i=1}^{N} Z_i \tag{13}$$

where N is the total data points and Zi = $\Delta c_{HbO}(t)$, across every data point.

(SK) Signal Skewness was derived from the dissymmetry of signal mean corresponding to its normal distribution:

$$Skew(Z) = E\left[\left(\frac{Z-\mu}{\sigma}\right)^3\right] \tag{14}$$

where E is predicted value of Z and standard deviation of Z is defined by σ.

(KR) Kurtosis was computed as:

$$Kurt(Z) = E\left[\left(\frac{Z-\mu}{\sigma}\right)^4\right] \tag{15}$$

where E is predicted value of Z and standard deviation of Z is defined by σ

(SD) Standard Deviation computed by applying *Polyfit* function in which data points are fitted with a line in MATLAB®.

SP Signal Peak is determined by applying the *max* function in MATLAB®.

These above features are normalized using:

$$x' = \frac{x - \min(x)}{\max(x) - \min(x)} \tag{16}$$

where $x'$is the output value rescaled, $x \in R^N$ denotes feature values, the smallest value is denoted by $\min(x)$, and the highest value is $\max(x)$. Fig. 7 shows the plot of subject one for all six features before the normalization.

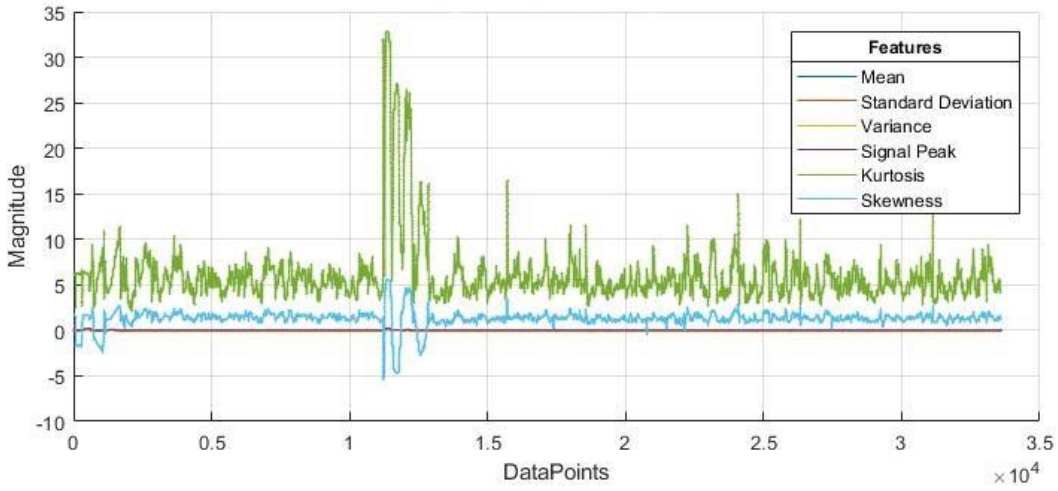

Figure 22. Plot of Six Statistical Feature

4.7.1 Mel Frequency Cepstral Coefficient (MFCC)

Mel frequency cepstral coefficients (MFCCs) are commonly used for the identification of automatic speakers. Davis and Mermelstein launched them in the 1980's and have been cutting-edge ever since [73].

In order to explain it in simple words, we presume that the fNIRS signal which is also a time domain signal like audio signal does not change significantly on short time scales (if we say it doesn't change, statistically, this means statistically stable, obviously, the samples change continuously in even very short time scales). Therefore, we windowed the signal into short frames from 20 to 40ms. When the frame is much shorter, we do not get the enough measurements, to get accurate spectral approximation.

The next move is to determine each frame's power spectrum. This is triggered by the human cochlea (an ear organ), which vibrates at various points in accordance with the frequency of the incoming sounds. Dept nerve fire reminding the brain that other frequencies are present based on the location in the vibratory cochlea (which wobbles small hair). Our periodogram estimation does a related function for us, which defines the frequencies in the picture.

The cochlea cannot differentiate between two frequencies which are closely spaced. This influence improves with elevated frequencies. That is why we use clumps of periodogram

containers to get an insight into how much energy occurs in specific frequency regions. The first filter is very small and shows how much energy is around 0 hertz. That will be achieved by our Mel filter-bank. When frequencies increase, our filters become wider when differences become less significant. We just want to know about the amount of energy that occurs in any location

We take the logarithm of the filter bank energies. That is guided by our ears, too: on a linear scale we do not detect loudness. In fact, we have to apply eight times as much energy to double the perceived amplitude of a signal. It means the major energy variations cannot sound so distinctive when the sound starts loud. This encoding process makes our features more in line with what people say. The logarithm permits one to use cepstral mean subtraction, a technique used to normalize the signal.

The last step is to evaluate the DCT of the energy from the log filter stack. It's done for two primary reasons. Owing to the similarity of our filter banks, the filter bank energies are well correlated. The DCT decorates the energy that allows diagonal covariance matrices to be used for modeling the characteristics of a classifier, for example. Note that out of the 26 DCT coefficients, only 12 are preserved. The explanation would be that the larger DCT coefficients reflect rapidly changing energy in a filter bank, and it turns out how these fast changes are actually degrading speech recognition efficiency.

MFCCs of fNIRS signal can be extracted by using following steps.

- Divide the signal into windows of 25ms frames. If you cannot split the signal into an even number of windows, pad it with zeros.
- Calculate the Discrete Fourier Transform (DCT) of a windowed signal using the following equation.

$$S_i(k) = \sum_{n=1}^{N} s_i(n)h(n)e^{-\frac{j2\pi kn}{N}} \quad 1 \leq k \geq K \tag{17}$$

Where

$s_i(n)$ is a time domain signal frame i

$s_i(k)$ is a DFT of frame i

$h(n)$ is an analysis window of the signal

K is the length of DFT

The power spectral estimate for the signal frame is given by:

$$P_i(k) = \frac{1}{N}|s_i(k)|^2 \tag{18}$$

We perform the 512-point FFT and keep only 257 coefficients.

- Convert the powers of spectrum into Mel scale using Mel filter bank. A range of 20–40 triangular filters in which 26 are standard for power spectral approximation of power. The 26 vectors with length of 257 as selected in FFT settings in above step are available in our filter bank. We multiply each bank with the power spectrum and then sum up the coefficients to determine filter bank energies. Once that is completed, we have 26 numbers that remind us how much energy each filter bank has. Figure 23 shows hopefully clear the basic concept of this how this step is done.

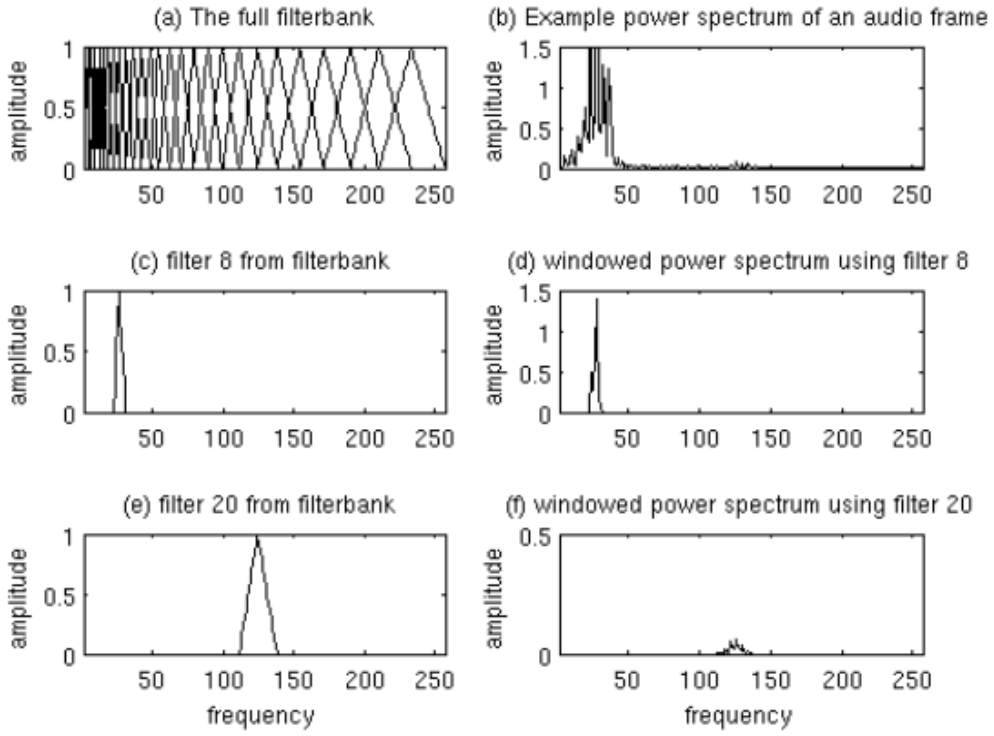

Figure 23. Plot to calculate the Mel filter Bank [74]

- Calculate the log power of each of 26 Mel frequencies which leaves us with 26 energies from the previous step.
- Calculate the discrete cosine transform (DCT) of 26 log filter bank energies to give us the 26 cepstral coefficients.
- We keep 12-13 coefficients and rest are discarded due to the reason explained above. These 12-13 features are called frequency Cepstral Coefficients.

4.8 Classification

Three classifier LDA, SVM and KNN are used for the classification in which the statistical features and MFCC features are used separately. K fold cross validation is implemented to acquire the perfect classification accuracy with 10 different settings of test and train datasets.

5. Results and Discussion

5.1 Results

The classification performance was evaluated by 10-fold cross-validation followed by each classifier over the course of 10 runs. In 10-fold cross-validation, the original sample is randomly partitioned into 10 equal sized subsamples. Of the 10 subsamples, a single subsample is retained as the validation data for testing the performance or accuracy, and the remaining k-1 subsamples are used as training data.

5.1.1 Using Statistical Feature

The classification accuracy of using the statistical features in time domain are shown in confusion matrix representation in which classifications accuracy of each subject with each classifier is shown.

Classification of each subject using KNN classifier is shown below.

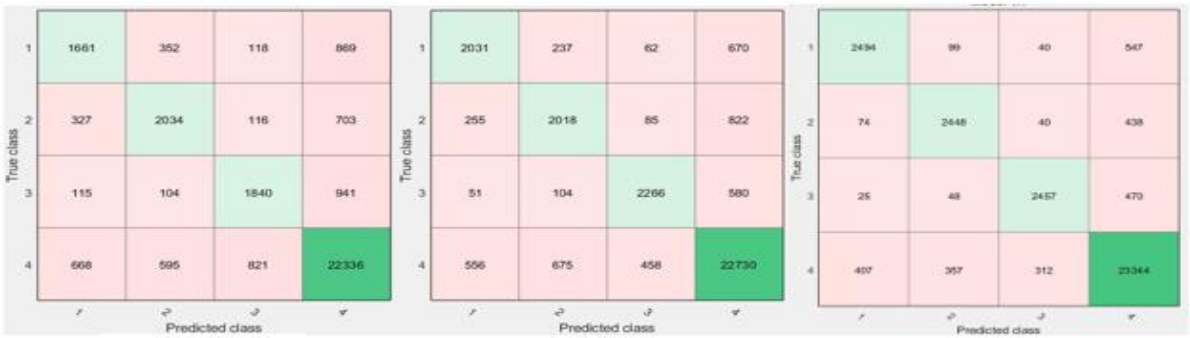

S01 S02 S03

S04 S05

Classification of each subject using LDA classifier is shown below

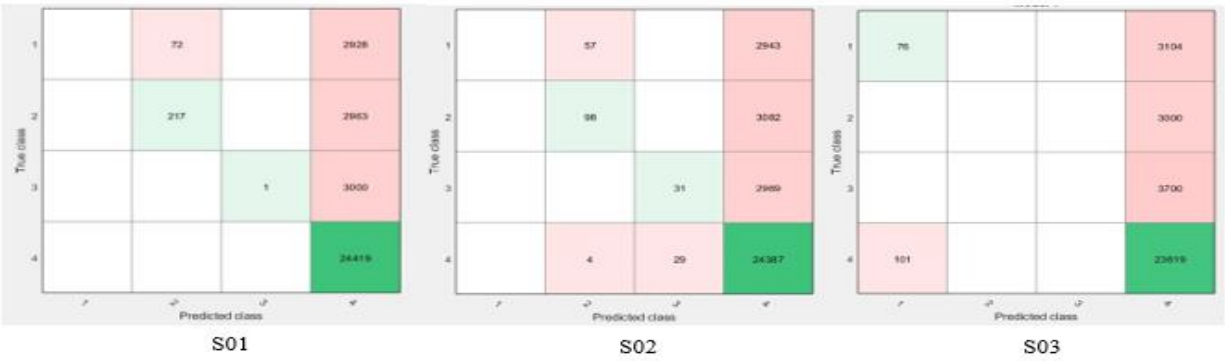

S01 S02 S03

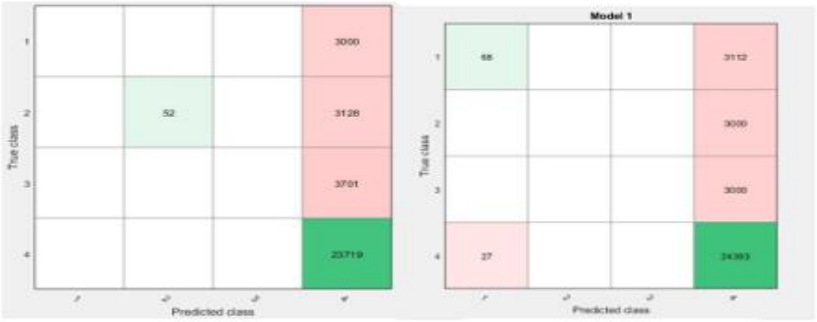

S04 S05

Classification of each subject using SVM classifier is shown below:

S01 S02 S03

S04 S05

The results of four class classification is shown in the Table shows that the maximum accuracy we have achieved using six statistical features simultaneously is by using a nonlinear classifier KNN which is greater than 90%.

Table 2. Accuracy using Six Statistical Features

Subjects	**LDA %**	**KSVM %**	**KNN %**
S01	72.67	75.6	91.5
S02	73.51	75.4	89.4
S03	73.51	76.4	90.9
S04	70.59	74.2	93.5
S05	70.59	75.5	87.4
Average	72.15	75.42	90.54

5.1.2 Using MFCC

We use two techniques as mentioned earlier to find the MFCC than the optimal classification accuracy of four class BCI system. The result is obtained using the first technique which is calculating MFCC features after vector averaging is shown in table below.

Table 3. Accuracy Using MFCC Features with Vectors Averaging

Subjects	**LDA %**	**KSVM %**	**KNN %**
S01	96.25	92.5	52.5
S02	96.25	91.25	35
S03	95	91.25	50
S04	95	93.25	45
S05	96.25	93.25	25
Average	**95.75**	**92.30**	**41.25**

The results using second technique which is obtaining the MFCC features of each class after channel averaging is shown in table below.

Table 4. Accuracy Using MFCC with Channel Averaging

Subjects	LDA %	KSVM %	KNN %
S01	73.75	91.25	45
S02	75	93.75	50
S03	76.25	85	50
S04	67.5	87.5	32.5
S05	77.5	90	47.5
Average	**74**	**89.5**	**45**

5.2 Discussion

In this fact-finding analysis we are successfully able to analyze and enhance the classification accuracy by utilizing the fNIRS data of 5 subjects from open access dataset [75]. As the overall data is of 4 class i.e. LHMI, RHMI, MA and Rest but taken separately in pairs. Per pair of data consist of 2 class so data is converted into 4 class by joining the 2 separated pair of data i.e. LHMI vs RHMI, MA vs Rest to LHMI vs RHMI vs MA vs Rest. In the literature using this dataset no such type of study is performed but separately i.e. MI vs Rest and MA vs Rest. The maximum classification accuracies they achieved in MA vs Rest task using the Hilton transform and sum derivative as a feature with KNN are 82.87% and 84.94% respectively which are pretty low as compare to this study [76]. In another study of MI vs Rest NIRS with Common Spatial Pattern (CSP) shows the classification accuracy of as high as 71.4% with (LSVM) linear support vector machine classifier and for the NIRS with Time Domain Parameters (TDP) and only NIRS features they get the mean accuracies of 50.5% and 53.1% by using Kernel SVM (KSVM) which is also for less than the accuracies we get with KSVM [77].

Furthermore, previous fNIRS based BCI research have mostly used advance methods of signal processing and novel method of feature selection algorithm and advance classifier to

improve the classification accuracy and therefore enhancing the performance. This study emphasized on improving the classification accuracy using the set of simple time domain statistical feature as well as a novel technique of using MFCC features and then comparing the results of both the features by classifying them using 3 different classifiers from basic linear classifier LDA to moderate kernel SVM to advance nonlinear classifier KNN.

Table 5 provides a summary of most studies that demonstrated accuracy of four-class fNIRS-BCI

Table 5. Summary of Four Class fNIRS-BCI Studies

Reference	*Features*	*Classifier*	*Accuracy (%)*
Khan et al. (2014)	Mean	LDA	>80
Hong et al. (2015)	Mean, Slope	Multiclass LDA	75.6
Naseer and Hong (2015)	Mean & Slope	LDA	73.3
Yin et al. (2016)	Difference HbO & HbR	ELM	>75
Buccino et al (2016)	CSP	LDA	>70
Qureshi et al. (2017)	**Peak, Slope**	**SVM**	**87.8**
Zafer et al. (2017)	Mean, Min, Skew	LDA	73.2
Erdogan et al (2019)	**Mean, Peak, Skewness, Slope, Kurtosis, SD**	**ANN**	**94**
This Research	**Statistical Feature**	**KNN**	**90.54**
	MFCC Features	**LDA**	**95.75**

The benchmark paper which is selected based on the four-class system in which motor imagery and mental arithmetic is performed as performed in this study is used to compare the improved accuracies. The finding of bench mark paper used Generalized Linear Model approach to enhance the classification accuracy of the system to 87.5% [70].

While comparing the result of this study with the bench mark paper as shown by the data in the above tables we can clearly see that using the statistical features with nonlinear classifier

such as KNN shows the classification accuracy of greater than 90 percent than the linear classifier LDA and SVM.

While comparing the results of MFCC features to the bench mark paper in which LDA is used which is a linear classifier the result is pretty lower than the result we have obtained. Moreover, by comparing the overall result shows that the MFCC features calculated after vector averaging shows the highest improvement in accuracy of four class fNIRS BCI system.

6. Conclusion and Future Work

6.1 Conclusion

After the extensive and detailed result-oriented research following conclusion can be drawn. Increasing the number of physiological channels will increase the data captured by the electrode which is a plus point but it also captures the irrelevant data artifact and noise. Using the HbO signal rather than the HbR signal increases the chances of improving the classification accuracy of fNIRS BCIs. Data synchronization can be done if the data is collected with the same machine, sampling rate at the same time with the same participant but with different task at different intervals. Simple filters with optimal values for preprocessing can be used to enhance the classification accuracy rather going for the complex ones. Maximum number of statistical features in time domain directly increase the classification accuracy. For further enhancement frequency domain features like MFCC and advance feature selection techniques can be used. Classifier plays an important role in enhancing the classification accuracy when used with the optimal features as seen from the result KNN a nonlinear classifier gives the higher accuracy while using the statistical feature while LDA and SVM gives the highest accuracy using MFCC features.

6.2 Future Recommendation

Using the MFCC features gives the best promising classification accuracy so far as compare to the most of the research using more than two commands. However future work can be done in following areas of this research.

- A hybrid approach can be developed by using statistical features as well as MFCC features combine and then best feature selection algorithm is applied to select the best compatible features to further enhance the classification accuracy.
- Rasta, PLP and both combine features can be used to calculate the enhanced classification results which are used in speech recognition and are more sophisticated techniques in enhancing classification.
- Artificial Neural Network (ANN) can be trained the using the MFCC features.

REFERENCES

[1] "Wolpaw, J. R., Birbaumer, N., McFarland, D. J., Pfurtscheller, G., & Vaughan, T. M. (2002). Brain–computer interfaces for communication and control. Clinical neurophysiology, 113(6), 767-791.".

[2] "Ortner, R., Allison, B. Z., Korisek, G., Gaggl, H., & Pfurtscheller, G. (2011). An SSVEP BCI to control a hand orthosis for persons with tetraplegia. IEEE Transactions on Neural Systems and Rehabilitation Engineering, 19(1), 1-5.".

[3] "Vaughan, T. M., Heetderks, W. J., Trejo, L. J., Rymer, W. Z., Weinrich, M., Moore, M. M., ... & Wolpaw, E. W. (2003). Brain-computer interface technology: a review of the Second International Meeting.".

[4] "Kübler, A., Kotchoubey, B., Kaiser, J., Wolpaw, J. R., & Birbaumer, N. (2001). Brain–computer communication: Unlocking the locked in. Psychological bulletin, 127(3), 358.".

[5] "Thakor, N. V. (2013). Translating the brain-machine interface. Science translational medicine, 5(210), 210ps17-210ps17.".

[6] "Schwartz, A. B. (2004). Cortical neural prosthetics. Annu. Rev. Neurosci., 27, 487-507.".

[7] "Lebedev, M. A., & Nicolelis, M. A. (2006). Brain–machine interfaces: past, present and future. TRENDS in Neurosciences, 29(9), 536-546.".

[8] "Wolpaw, J. R., & McFarland, D. J. (2004). Control of a two-dimensional movement signal by a noninvasive brain-computer interface in humans. Proceedings of the national academy of sciences, 101(51), 17849-17854.".

[9] "M. Mauro et al. “Spatial attention orienting to improve the efficacy of a brain-computer interface for communication,” in Proceedings of the 9th ACM SIGCHI Italian Chapter International Conference on Computer Human Interaction, 2011.".

[10] "Gharagozlou, F. , et al. (2015). Detecting driver mental fatigue based on EEG alpha power changes during simulated driving. Iranian journal of public health, 44(12), 1693".

[11] "Halder, S., Pinegger, A., Käthner, I., Wriessnegger, S. C., Faller, J., Antunes, J. B. P., ... & Kübler, A. (2015). Brain-controlled applications using dynamic P300 speller matrices. Artificial intelligence in medicine, 63(1), 7-17.".

[12] "Zhang, R. et al (2016). Control of a wheelchair in an indoor environment based on a brain–computer interface and automated navigation. IEEE transactions on neural systems and rehabilitation engineering, 24(1), 128-139.".

[13] "Belkacem, A. N., Saetia, S., Zintus-art, K., Shin, D., Kambara, H., Yoshimura, N., ... & Koike, Y. (2015). Real-time control of a video game using eye movements and two temporal EEG sensors. Computational intelligence and neuroscience, 2015, 1.".

[14] "Abdulkader, S. N., Atia, A., & Mostafa, M. S. M. (2015). Brain computer interfacing: Applications and challenges. Egyptian Informatics Journal, 16(2), 213-230.".

[15] "van Erp, J., Lotte, F., & Tangermann, M. (2012). Brain-computer interfaces: beyond medical applications. Computer, 45(4), 26-34.".

[16] "Rao, R. P., & Scherer, R. (2010). Brain-computer interfacing [in the spotlight]. IEEE Signal Processing Magazine, 27(4), 152-150.".

[17] "Samek, W., Müller, K. R., Kawanabe, M., & Vidaurre, C. Brain-computer interfacing in discriminative and stationary subspaces. In Engineering in Medicine and Biology Society (EMBC), 2012 Annual International Conference of the IEEE (pp. 2873-2876). IEEE.".

[18] "Wang, Y., & Jung, T. P. (2012). Improving brain–computer interfaces using independent component analysis. In Towards Practical Brain-Computer Interfaces (pp. 67-83). Springer, Berlin, Heidelberg.".

[19] "Umair, Aroosa & Ashfaq, Ureeba & Gufran Khan, Muhammad. (2017). Recent Trends, Applications, and Challenges of Brain-Computer Interfacing (BCI). International Journal of Intelligent Systems and Applications. 9. 58-65. 10.5815/ijisa.2017.02.08."

[20] "Ulaş, Ç. (2013). Incorporation of a language model into a brain computer interface-based speller (Doctoral dissertation, Doctoral dissertation, Sabancı University).".

[21] "Ramadan, R. A., Refat, S., Elshahed, M. A., & Ali, R. A. (2015). Basics of brain computer interface. In Brain-Computer Interfaces (pp. 31-50). Springer, Cham.".

[22] "Rao, T. K., Lakshmi, M. R., & Prasad, T. V. (2012). An exploration on brain computer interface and its recent trends. arXiv preprint arXiv:1211.2737.".

[23] Parasuraman, R., & Rizzo, M. (2008). Introduction to neuroergonomics. OXFORD SERIES IN HUMAN-TECHNOLOGY INTERACTION, 1..

[24] "Yadava, M., Kumar, P., Saini, R., Roy, P. P., & Dogra, D. P. (2017). Analysis of EEG signals and its application to neuromarketing. Multimedia Tools and Applications, 76(18), 19087-19111.".

[25] "Geeta, N., & Gavas, R. D. (2014). Enhanced learning with Abacus and its analysis using BCI Technology. International Journal of Modern Education and Computer Science, 6(9), 22.".

[26] "Lécuyer, A., Lotte, F., Reilly, R. B., Leeb, R., Hirose, M., & Slater, M. (2008). Brain-computer interfaces, virtual reality, and videogames. Computer, 41(10).".

[27] "Chuang, J., Nguyen, H., Wang, C., & Johnson, B. (2013, April). I think, therefore i am: Usability and security of authentication using brainwaves. In International Conference on Financial Cryptography and Data Security (pp. 1-16).".

[28] "Fan, X. A., Bi, L., & Wang, Z. (2012, July). Detecting emergency situations by monitoring drivers' states from EEG. In Complex Medical Engineering (CME), 2012 ICME International Conference on (pp. 245-248). IEEE.".

[29] "Paulraj, M. P. et al(2012, September). EEG based hearing perception level estimation for normal hearing persons. In Control, Systems & Industrial Informatics (ICCSII), 2012 IEEE Conference on (pp. 160-162). IEEE.".

[30] "Bagchi, S., & Chattopadhyay, M., An easy-to-adopt approach for regular and routine monitoring of the consciousness level of human brain of stayed alone sick person. In Sensing Technology (ICST), 2012 Sixth International Conference on (pp. 698-703) IEEE.".

[31] "Widyotriatmo, A., & Andronicus, S. (2015, May). A collaborative control of brain computer interface and robotic wheelchair. In Control Conference (ASCC), 2015 10th Asian (pp. 1-6). IEEE.".

[32] "Velasco-Álvarez, F., Fernández-Rodríguez, Á., Díaz-Estrella, A., Blanca-Mena, M. J., & Ron-Angevin, R. (2018). Control strategies of a brain-controlled wheelchair using two mental tasks. In Smart Wheelchairs and Brain-Computer Interfaces (pp. 345-368).".

[33] "Allison, B. Z., Wolpaw, E. W., & Wolpaw, J. R. (2007). Brain–computer interface systems progress and prospects. Expert review of medical devices, 4(4), 463-474.".

[34] "Allison, B., Graimann, B., & Gräser, A. (2007, June). Why use a BCI if you are healthy. In ACE Workshop-Brain-Computer Interfaces and Games (pp. 7-11).".

[35] "Pfurtscheller, G., Neuper, C., Muller, G. R., Obermaier, B., Krausz, G., Schlogl, A., ... & Wortz, M. (2003). Graz-BCI state of the art and clinical applications. IEEE Transactions on neural systems and rehabilitation engineering, 11(2), 1-4.".

[36] "Riehle, A. (2005). Preparation for action one of the key functions of the motor cortex. Motor cortex in voluntary movements A distributed system for distributed functions, 33, 213-240.".

[37] "Khan, M. J., & Hong, K. S. (2015). Passive BCI based on drowsiness detection: an fNIRS study. Biomedical optics express, 6(10), 4063-4078.".

[38] "Curran, E. A., & Stokes, M. J. (2003). Learning to control brain activity a review of the production and control of EEG components for driving brain–computer interface (BCI) systems. Brain and cognition, 51(3), 326-336.".

[39] Schalk, Gerwin., and Jürgen Mellinger., A Practical Guide to Brain–Computer Interfacing with BCI2000: General-Purpose Software for Brain-Computer Interface Research, Data Acquisition, Stimulus Presentation, and Brain Monitoring, Springer Science & Business Media, 2010.

[40] Finke C, Kopp UA, Scheel M, Pech LM, Soemmer C, Schlichting J, Leypoldt F, Brandt AU, Wuerfel J, Probst C, Ploner CJ, Functional and structural brain changes in anti–N-methyl-D-aspartate receptor encephalitis, Annals of neurology, 74(2), 2013.

[41] Ye JC, Tak S, Jang KE, Jung J, Jang J, NIRS-SPM: statistical parametric mapping for near-infrared spectroscopy, Neuroimage, 44(2), 428-47, 2009.

[42] Gui, X. U. E., C. H. E. N. Chuansheng., L. U. Zhong-Lin., and D. O. N. G. Qi., Brain imaging techniques and their applications in decision-making research, Xin li xue bao. Acta psychologica Sinica 42, 2010, 120.

[43] https://en.wikipedia.org/wiki/Magnetoencephalography

[44] http://web-japan.org/trends/09_sci-tech/sci090319.html

[45] Enzinger, Christian., Stefan, Ropele., Franz, Fazekas., Marisa, Loitfelder., Faton, Gorani., Thomas, Seifert., Gudrun, Reiter., Christa, Neuper., Gert, Pfurtscheller., and Gernot, Müller-Putz., Brain motor system function in a patient with complete spinal cord injury following

extensive brain–computer interface training, Experimental Brain Research 190, 2008, 215-223.

[46] http://www.slideshare.net/RoxMae/electroencephalogram-electroencephalography

[47] Coyle, Shirley., Tomás, Ward., Charles, Markham., and Gary, McDarby., On the suitability of near-infrared (NIR) systems for next-generation brain–computer interfaces, Physiological Measurement 25, 2004, 815.

[48] Naseer, Noman., and Keum-Shik Hong., fNIRS-based brain-computer interfaces: a review, Frontiers in Human Neuroscience, Switzerland, January, 3, 2015.

[49] Delpy, David T., Mark, Cope., Pieter van der Zee., S, R, Arridge., Susan, Wray., and J, S, Wyatt., Estimation of optical pathlength through tissue from direct time of flight measurement, Physics in Medicine and Biology 33, 1988, 1433.

[50] Jobsis, Frans F., Noninvasive, infrared monitoring of cerebral and myocardial oxygen sufficiency and circulatory parameters, Science 198, 1977, 1264-1267.

[51] Villringer, Arno., J. Planck., C. Hock., L. Schleinkofer., and U. Dirnagl., Near infrared spectroscopy (NIRS): a new tool to study hemodynamic changes during activation of brain function in human adults, Neuroscience letters154, 1993, 101-104.

[52] Naseer, Noman., and Hong, Keum-Shik., Classification of functional near-infrared spectroscopy signals corresponding to the right-and left-wrist motor imagery for development of a brain–computer interface, Neuroscience Letters 553, 2013, 84- 89.

[53] http://www.jarrodmillman.com/rcsds/lectures/convolution_background.html

[54] Sassaroli, Angelo., and Sergio, Fantini., Comment on the modified Beer–Lambert law for scattering media, Physics in Medicine and Biology 49, 2004, N255.

[55] https://en.wikipedia.org/wiki/Feature_selection

[56] Naseer, Noman., Qureshi, Nauman Khalid., Noori, Farzan Majeed., and Hong, Keum-Shik., Analysis of different classification techniques for two-class functional near-infrared spectroscopy-based brain-computer interface, Computational Intelligence and Neuroscience, Hindawi (In Press).

[57] Duda, R. O., Hart, P. E., & Stork, D. G. (2012). Pattern classification. John Wiley & Sons.

[58] Fukunaga, K. (2013). Introduction to statistical pattern recognition. Elsevier

[59] "Burges, C. J. (1998). A tutorial on support vector machines for pattern recognition. Data mining and knowledge discovery, 2(2), 121-167.".

[60] "Müller, K. R., Krauledat, M., Dornhege, G., Curio, G., & Blankertz, B. (2004). Machine learning techniques for brain-computer interfaces.".

[61] Berdakh Abibullaev, Jinung An. Classification of frontal cortex hemodynamic responses during cognitive tasks using wavelet transforms and machine learning algorithms. Medical engineering & physics 34, 2012, 1394-1410.

[62] Hai Thanh Nguyen, Cuong Quoc Ngo, KHOA Truong Quang Dang, Van Toi Vo Temporal hemodynamic classification of two hands tapping using functional near—infrared spectroscopy, Frontiers in human neuroscience, 7, 2013, 516.

[63] Classification of functional near-infrared spectroscopy signals corresponding to the right- and left-wrist motor imagery for development of a brain–computer interface, N Naseer, KS Hong, Neuroscience letters 553, 84-89

[64] N. Naseer, K.-S. Hong, Classification of functional near-infrared spectroscopy signals corresponding to the right- and left-wrist motor imagery for development of a brain–computer interface, Neuroscience. Lett. (2013)

[65] KS Hong, N Naseer, YH Kim, Classification of prefrontal and motor cortex signals for three-class fNIRS–BCI, Neuroscience letters 587, 87-92

[66] N Naseer, FM Noori, NK Qureshi, KS Hong, Determining optimal feature-combination for LDA classification of functional near-infrared spectroscopy signals in brain-computer interface application, Frontiers in human neuroscience 10, 237

[67] NK Qureshi, FM Noori, A Abdullah, N Naseer, Comparison of classification performance for fNIRS-BCI system, 2016 2nd International Conference on Robotics and Artificial Intelligence (ICRAI)

[68] N Naseer, FM Noori, NK Qureshi, KS Hong. “Determining optimal feature-combination for LDA classification of functional near-infrared spectroscopy signals in brain-computer interface application”, Frontiers in human neuroscience 10, 237

[69] KS Hong, N Naseer, “Reduction of delay in detecting initial dips from functional near-infrared spectroscopy signals using vector-based phase analysis”, International Journal of Neural Systems 26 (03), 1650012

[70] NK Qureshi, N Naseer, FM Noori, H Nazeer, RA Khan, S Saleem, Enhancing classification performance of functional near-infrared spectroscopy-brain–computer interface using adaptive estimation of general linear model coefficients, Frontiers in neurorobotics 11, 33

[71] FM Noori, N Naseer, NK Qureshi, H Nazeer, RA Khan, Optimal feature selection from fNIRS signals using genetic algorithms for BCI, Neuroscience letters 647, 61-66

[72] RA Khan, N Naseer, NK Qureshi, FM Noori, H Nazeer, MU Khan, fNIRS-based Neurorobotic Interface for gait rehabilitation, Journal of neuroengineering and rehabilitation 15 (1), 7

[73] Davis, S. Mermelstein, P. (1980) Comparison of Parametric Representations for Monosyllabic Word Recognition in Continuously Spoken Sentences. In IEEE Transactions on Acoustics, Speech, and Signal Processing, Vol. 28 No. 4, pp. 357-366

[74] X. Huang, A. Acero, and H. Hon. Spoken Language Processing: A guide to theory, algorithm, and system development. Prentice Hall, 2001.

[75] J. Shin et al., "Open Access Dataset for EEG+NIRS Single-Trial Classification," in IEEE Transactions on Neural Systems and Rehabilitation Engineering, vol. 25, no. 10, pp. 1735-1745, Oct. 2017.

[76] E. Ergün and Ö. Aydemir, "Decoding of Binary Mental Arithmetic Based Near-Infrared Spectroscopy Signals," 2018 3rd International Conference on Computer Science and Engineering (UBMK), Sarajevo, 2018, pp. 201-204.

[77] H. Kim, I. Wang, Y. Kim, H. Kim and D. Kim, "Comparative Analysis of NIRS-EEG Motor Imagery Data Using Features from Spatial, Spectral and Temporal Domain," 2020 8th International Winter Conference on Brain-Computer Interface (BCI), Gangwon, Korea (South), 2020, pp. 1-4.

APPENDIX A

Matlab Code:

```
%%---------------------------------- Loading Data-------------------------------------------%

clear all;
load ('C:\Users\saadg\Desktop\MFCC\subject 05\cnt.mat')

%% ----------------------Synchronizing Data to make 4 Classes---------------------------%

%%%%%%%%%%%%%%%%%%%%%%%%%%%%%%%%%%%%%%%%%%%%
%-------------------------Cnt.mat contain the data in as following---------------------------%
% -------------------cnt: 1x6 cells, continuous NIRS light intensity data--------------------%
%-------------------cnt{1,1}, cnt{1,3}, cnt{1,5}: DATA for motor imagery.------------------%
%-------------------cnt{1,2}, cnt{1,4}, cnt{1,6}: DATA for mental arithmetic----------------%
%%%%%%%%%%%%%%%%%%%%%%%%%%%%%%%%%%%%%%%%%%%%

%----------------------STEP 1: Saving the data Separately into Variables-------------------%
a=cnt{1, 1}.x;
b=cnt{1, 2}.x;
c=cnt{1, 3}.x;
d=cnt{1, 4}.x;
e=cnt{1, 5}.x;
f=cnt{1, 6}.x;

%-------STEP 2a: Dividing the MI data into Trails and Saving it to separately in Cells-------%
X1 = ones(560,72);
MI1 = cell(1,10);
O=10;
```

```
N1=224;
for i=1:O
   X1(:,:)= a(1+N1:560+N1,:);
   MI1{i} = X1;
   N1=560*i;
end
MI2 = cell(1,10);
O=10;
N1=224;
for i=1:O
   X1(:,:)= c(1+N1:560+N1,:);
   MI2{i} = X1;
   N1=560*i;
end
MI3 = cell(1,10);
O=10;
N1=224;
for i=1:O
   X1(:,:)= e(1+N1:560+N1,:);
   MI3{i} = X1;
   N1=560*i;
end

%------------STEP 2b : Combing 3 separate runs of MI data into Single Variable----------------%
MI=[MI1,MI2,MI3];

%-------STEP 3a: Dividing the MA data into Trails and Saving it to separately in Cells-------%
X1 = ones(560,72);
MA1 = cell(1,10);
```

```
O=10;
N1=224;
for i=1:O
   X1(:,:)= b(1+N1:560+N1,:);
   MA1{i} = X1;
   N1=560*i;
end
MA2 = cell(1,10);
O=10;
N1=224;
for i=1:O
   X1(:,:)= d(1+N1:560+N1,:);
   MA2{i} = X1;
   N1=560*i;
end
MA3 = cell(1,10);
O=10;
N1=224;
for i=1:O
   X1(:,:)= f(1+N1:560+N1,:);
   MA3{i} = X1;
   N1=560*i;
end
%------------STEP 3b : Combing 3 separate runs of MA data into Single Variable----------------%
MA=[MA1,MA2,MA3];
```

```
%--------------------STEP 4: Combining Both MI and MA data Channel Wise--------------------%
MIA=[];
for k=1:30
      MIA=[MIA;MI{1,k};MA{1,k}];
end

%------------------------STEP 5: Now Saving only HBO Data in a new Variable ----------------%
HbO=MIA(:,1:36);

%% -------------------------------------Data Preprocessing-----------------------------------------%%

%--------------Filter Design Data----------------------%
Fs = 10;                        % Sampling Frequency (Hz)
Fn = Fs/2;                      % Nyquist Frequency (Hz)
n = 6;                          % Order of Filter
%--------------Design Low Pass Filter-------------------%
Fco = 0.3;                        % Cutoff Frequency (Hz)
Wn = Fco/Fn;                    % Normalised Cutoff Frequency (rad)
[b,a] = butter(n,Wn,'low');     % Designs lowpass Filter By Default
HbOO = filter (b,a,HbO);        %Applying Low Pass Filter
%--------------Design High Pass Filter------------------%
Fcoh = 0.01;                    % Cutoff Frequency (Hz)
Wp = Fcoh/Fn;                   % Normalised Cutoff Frequency (rad)
[b,a] = butter(n,Wp,'high');    % Designs Highpass Filter By Default
HBO= filter (b,a,HbOO);         %Applying High Pass Filter
%---------------Saving as CSV File----------------------%
HBO=array2table(HBO);           %Coverting the array data to table form
writetable(HBO,'S05.csv');      %Saving it in CSV File
```

Python Code:

```
#-----------------------------------Importing Libraries---------------------------#
import numpy as np
import matplotlib.pyplot as plt
plt.figure
import pandas as pd
import librosa

#------------------------------ Importing the CSV File-----------------------------#
dataset = pd.read_csv('S05.csv')

#----------------Extracting the class 1 data points (Intervals)----------------------#
Trail1=dataset.loc[0:99,:]
Trail2=dataset.loc[1120:1219,:]
Trail3=dataset.loc[2240:2339,:]
Trail4=dataset.loc[3360:3459,:]
Trail5=dataset.loc[4760:4859,:]
Trail6=dataset.loc[5600:5699,:]
Trail7=dataset.loc[6720:6819,:]
Trail8=dataset.loc[7840:7939,:]
Trail9=dataset.loc[8960:9059,:]
Trail10=dataset.loc[10360:10459,:]
Trail11=dataset.loc[11200:11299,:]
Trail12=dataset.loc[12320:12419,:]
Trail13=dataset.loc[13440:13539,:]
Trail14=dataset.loc[14840:14939,:]
Trail15=dataset.loc[15680:15779,:]
Trail16=dataset.loc[16800:16899,:]
Trail17=dataset.loc[17920:18019,:]
```

```
Trail18=dataset.loc[19320:19419,:]
Trail19=dataset.loc[20160:20259,:]
Trail20=dataset.loc[21560:21659,:]
Trail21=dataset.loc[22400:22499,:]
Trail22=dataset.loc[23800:23899,:]
Trail23=dataset.loc[24920:25019,:]
Trail24=dataset.loc[25760:25859,:]
Trail25=dataset.loc[26880:26979,:]
Trail26=dataset.loc[28000:28099,:]
Trail27=dataset.loc[29400:29499,:]
Trail28=dataset.loc[30520:30619,:]
Trail29=dataset.loc[31640:31739,:]
Trail30=dataset.loc[32480:32579,:]

#--------------Combining the Class 1 data and taking the mean------------------------------#
Class1=np.concatenate((Trail1,Trail2,Trail3,Trail4,Trail5,Trail6,Trail7,Trail8,Trail9,Trail10,
                       Trail11,Trail12,Trail13,Trail14,Trail15,Trail16,Trail17,Trail18,Trail19,Trail20,
                       Trail21,Trail22,Trail23,Trail24,Trail25,Trail26,Trail27,Trail28,Trail29,Trail30, ))
Mean1=np.mean(Class1,axis=1)

#----------------------Extracting the class 2 data points (Intervals)-------------------------#
Trail1=dataset.loc[280:379,:]
Trail2=dataset.loc[1400:1499,:]
Trail3=dataset.loc[2520:2619,:]
Trail4=dataset.loc[3640:3739,:]
Trail5=dataset.loc[4480:4579,:]
Trail6=dataset.loc[5880:5979,:]
Trail7=dataset.loc[7000:7099,:]
Trail8=dataset.loc[7840:7939,:]
```

```
Trail9=dataset.loc[9240:9339,:]
Trail10=dataset.loc[10080:10179,:]
Trail11=dataset.loc[11200:11299,:]
Trail12=dataset.loc[12320:12419,:]
Trail13=dataset.loc[13720:13819,:]
Trail14=dataset.loc[14840:14939,:]
Trail15=dataset.loc[15960:16059,:]
Trail16=dataset.loc[17080:17179,:]
Trail17=dataset.loc[17920:18019,:]
Trail18=dataset.loc[19320:19419,:]
Trail19=dataset.loc[20440:20539,:]
Trail20=dataset.loc[21560:21659,:]
Trail21=dataset.loc[22680:22779,:]
Trail22=dataset.loc[23800:23899,:]
Trail23=dataset.loc[24920:25019,:]
Trail24=dataset.loc[26040:26139,:]
Trail25=dataset.loc[26880:26979,:]
Trail26=dataset.loc[28000:28099,:]
Trail27=dataset.loc[29120:29219,:]
Trail28=dataset.loc[30240:30339,:]
Trail29=dataset.loc[31360:31459,:]
Trail30=dataset.loc[32760:32859,:]

#--------------Combining the Class 2 data and taking the mean-------------------------------#
Class2=np.concatenate((Trail1,Trail2,Trail3,Trail4,Trail5,Trail6,Trail7,Trail8,Trail9,Trail10,
                       Trail11,Trail12,Trail13,Trail14,Trail15,Trail16,Trail17,Trail18,Trail19,Trail20,
                       Trail21,Trail22,Trail23,Trail24,Trail25,Trail26,Trail27,Trail28,Trail29,Trail30, ))
Mean2=np.mean(Class2,axis=1)
```

```
#----------------Extracting the class 3 data points (Intervals)----------------------#
Trail1=dataset.loc[840:939,:]
Trail2=dataset.loc[1960:2059,:]
Trail3=dataset.loc[2800:2899,:]
Trail4=dataset.loc[3920:4019,:]
Trail5=dataset.loc[5320:5419,:]
Trail6=dataset.loc[6160:6259,:]
Trail7=dataset.loc[7560:7659,:]
Trail8=dataset.loc[8400:8499,:]
Trail9=dataset.loc[9800:9899,:]
Trail10=dataset.loc[10640:10739,:]
Trail11=dataset.loc[11700:11799,:]
Trail12=dataset.loc[13160:13259,:]
Trail13=dataset.loc[14280:14379,:]
Trail14=dataset.loc[15120:15219,:]
Trail15=dataset.loc[16520:16619,:]
Trail16=dataset.loc[17640:17739,:]
Trail17=dataset.loc[18480:18579,:]
Trail18=dataset.loc[19880:19979,:]
Trail19=dataset.loc[20720:20819,:]
Trail20=dataset.loc[22120:22219,:]
Trail21=dataset.loc[23240:23339,:]
Trail22=dataset.loc[24360:24459,:]
Trail23=dataset.loc[25200:25299,:]
Trail24=dataset.loc[26320:26419,:]
Trail25=dataset.loc[27720:27819,:]
Trail26=dataset.loc[28560:28659,:]
```

```
Trail27=dataset.loc[29960:30059,:]
Trail28=dataset.loc[31080:31179,:]
Trail29=dataset.loc[32200:32299,:]
Trail30=dataset.loc[33320:33419,:]

#--------------Combining the Class 3 data and taking the mean------------------------------#
Class3=np.concatenate((Trail1,Trail2,Trail3,Trail4,Trail5,Trail6,Trail7,Trail8,Trail9,Trail10,
                       Trail11,Trail12,Trail13,Trail14,Trail15,Trail16,Trail17,Trail18,Trail19,Trail20,
                       Trail21,Trail22,Trail23,Trail24,Trail25,Trail26,Trail27,Trail28,Trail29,Trail30, ))
Mean3=np.mean(Class3,axis=1)

#-----------------Extracting the class 4 data points (Intervals)----------------------#
Trail1=dataset.loc[560:659,:]
Trail2=dataset.loc[1680:1779,:]
Trail3=dataset.loc[3080:3179,:]
Trail4=dataset.loc[4200:4299,:]
Trail5=dataset.loc[5040:5139,:]
Trail6=dataset.loc[6440:6539,:]
Trail7=dataset.loc[7280:7379,:]
Trail8=dataset.loc[8680:8779,:]
Trail9=dataset.loc[9520:9619,:]
Trail10=dataset.loc[10920:11019,:]
Trail11=dataset.loc[12040:12139,:]
Trail12=dataset.loc[12880:12979,:]
Trail13=dataset.loc[14000:14099,:]
Trail14=dataset.loc[15400:15499,:]
Trail15=dataset.loc[16240:16339,:]
Trail16=dataset.loc[17360:17459,:]
Trail17=dataset.loc[18760:18859,:]
```

```
Trail18=dataset.loc[19600:19699,:]
Trail19=dataset.loc[21000:21099,:]
Trail20=dataset.loc[21840:21939,:]
Trail21=dataset.loc[22960:23059,:]
Trail22=dataset.loc[24080:24179,:]
Trail23=dataset.loc[25480:25579,:]
Trail24=dataset.loc[26600:26699,:]
Trail25=dataset.loc[27440:27539,:]
Trail26=dataset.loc[28840:28939,:]
Trail27=dataset.loc[29680:29779,:]
Trail28=dataset.loc[30800:30899,:]
Trail29=dataset.loc[31920:32019,:]
Trail30=dataset.loc[33040:33139,:]

#--------------Combining the Class 4 data and taking the mean-------------------------------#
Class4=np.concatenate((Trail1,Trail2,Trail3,Trail4,Trail5,Trail6,Trail7,Trail8,Trail9,Trail10,
                       Trail11,Trail12,Trail13,Trail14,Trail15,Trail16,Trail17,Trail18,Trail19,Trail20,
                       Trail21,Trail22,Trail23,Trail24,Trail25,Trail26,Trail27,Trail28,Trail29,Trail30, ))
Mean4=np.mean(Class4,axis=1)

#------------------------- Computing MFCC features Class 1-------------------------------#
N=13
mfcc1 = np.array(Mean1, dtype=np.float64)
MFCC_Class1 = librosa.feature.mfcc(y=mfcc1, sr=10, n_mfcc=N)

#------------------------- Computing MFCC features Class 2-------------------------------#
mfcc2 = np.array(Mean2, dtype=np.float64)
MFCC_Class2 = librosa.feature.mfcc(y=mfcc2, sr=10, n_mfcc=N)
```

```
# -------------------------Computing MFCC features Class 3----------------------------#
mfcc3 = np.array(Mean3, dtype=np.float64)
MFCC_Class3 = librosa.feature.mfcc(y=mfcc3, sr=10, n_mfcc=N)

#------------------------- Computing MFCC features Class 4----------------------------#
mfcc4 = np.array(Mean4, dtype=np.float64)
MFCC_Class4 = librosa.feature.mfcc(y=mfcc4, sr=10, n_mfcc=N)

#-------------------------Combining all 4 Classes of MFCC Features-----------------#
X=np.vstack((MFCC_Class1,MFCC_Class2,MFCC_Class3,MFCC_Class4))
#X=X.transpose()

#---------------Labelling the classes Corresponds to the MFCC features---------------#
labelclass1=np.ones((1,N))
#labelclass1=np.vstack((MFCC_Class1,labelclass1))
labelclass2=np.ones((1,N)).dot(2)
#labelclass2=np.vstack((MFCC_Class2,labelclass2))
labelclass3=np.ones((1,N)).dot(3)
#labelclass3=np.vstack((MFCC_Class3,labelclass3))
labelclass4=np.ones((1,N)).dot(4)
#labelclass4=np.vstack((MFCC_Class4,labelclass4))
#FinalFeatMat=np.hstack((labelclass1,labelclass2,labelclass3,labelclass4))
Y=np.hstack((labelclass1,labelclass2,labelclass3,labelclass4))
Y=Y.transpose()

#---------------Classification with 10 fold Cross Validation-----------------#
cv=10
from sklearn.discriminant_analysis import LinearDiscriminantAnalysis
classifierLDA=LinearDiscriminantAnalysis(solver='svd')
```

```
from sklearn.model_selection import cross_val_score
scoresLDA = cross_val_score(classifierLDA, X, Y, cv=cv)
Best_accuracy_LDA=scoresLDA.mean()
from sklearn.neighbors import KNeighborsClassifier
classifierKNN = KNeighborsClassifier(n_neighbors = 5, metric = 'minkowski', p = 2)
scoresKNN = cross_val_score(classifierKNN, X, Y, cv=cv)
Best_accuracy_KNN=scoresKNN.mean()
from sklearn.svm import SVC
classifierSVM = SVC(C=10,kernel = 'linear', random_state = 0)
scoresSVM = cross_val_score(classifierSVM, X, Y, cv=cv)
Best_accuracy_SVM=scoresSVM.mean()
```